STARS

Electronic Theses and Dissertations, 2020-

2020

Investigations on the Use of Hyperthermia for Breast Cancer Treatment

Sreekala Suseela
University of Central Florida

STARS Citation

University of Central Florida

STARS
Showcase of Text, Archives, Research & Scholarship

INVESTIGATIONS ON THE USE OF HYPERTHERMIA FOR BREAST CANCER
TREATMENT

by

SREEKALA SUSEELA
B.Tech. Government Engineering College Palakkad, 2003
M.Tech. Cochin University of Science and Technology, 2010

A dissertation submitted in partial fulfillment of the requirements
for the degree of Doctor of Philosophy
in the Department of Electrical and Computer Engineering
in the College of Engineering and Computer Science
at the University of Central Florida
Orlando, Florida

Fall Term
2020

Major Professor: Parveen Wahid

ABSTRACT

Hyperthermia using electromagnetic energy has been proven to be an effective method in the treatment of cancer. Hyperthermia is a therapeutic procedure in which the temperature in the tumor tissue is raised above 42˚C without causing any damage to the surrounding healthy tissue. This method has been shown to increase the effectiveness of radiotherapy and chemotherapy. Radio frequencies, microwave frequencies or focused ultrasound can be used to deliver energy to the tumor tissue to attain higher temperatures in the tumor region for hyperthermia application.

In this dissertation the use of a near field focused (NFF) microstrip antenna array for the treatment of stage 1 cancer tumors in the breast is proposed. The antenna array was designed to operate at a resonant frequency of 2.45 GHz. A hemispherical two-layer model of breast consisting of fat and glandular tissue layer was considered. The tumor, of the size of a typical stage 1 cancer, was considered at different locations within the breast tissue. The permittivity and conductivity of the breast and tumor tissue were obtained from literature. For a specific location of the tumor, the NFF array is positioned outside the breast in front of the tumor. The radiation from the array is focused onto the tumor and raises the temperature of the tumor. Regardless of the position of the tumor, when placed at the right distance, the array produced a focused spot at the tumor without heating the surrounding healthy tissue. Different placement locations of the antenna array were studied to analyze the depth of the focused radiation region. The antenna array can be placed on a rotating arm allowing it to be moved around the breast based on the tumor location. Results for the power density distribution, specific absorption rate and temperature increase in the tumor and surrounding breast region are presented.

Dedicated to my loving husband, Thomas Papali and my cute little kids-Amal and Archana and

my loving Dad in heaven and my Mom and my whole family

ACKNOWLEDGMENTS

TABLE OF CONTENTS

LIST OF FIGURES

ix

x

LIST OF TABLES

CHAPTER 1: INTRODUCTION

Rapid technological advances in radio frequency, microwave technology and computational techniques have opened a new realm of new therapeutic and diagnostic methods. RF/ microwave frequencies find applications in areas such as cancer therapy, cardiology, surgery and diagnostic applications such as cancer detection, MRI and more. Electromagnetic signals have the advantages of low health risk, low cost to implement, low operational cost, easy to use, and user friendly [1]. Electromagnetic signals have the capability to be transmitted, guided and focused.

Bioelectromagnetics rely on the property of electromagnetic waves to transmit or receive without making a direct contact at the point of interest. Bioelectromagnetic applications are affected by the dielectric nature of the human body, body size and tissue properties. The lossy nature controls the penetration of electromagnetic fields into the body. The penetration of electromagnetic fields also depends on the applied frequency. At high frequencies, the field penetration to the interior of the body is less, while the penetration is more at low frequencies. But at low frequencies the fields are not focused or localized.

1.1. Biomedical applications of Radiofrequencies and microwave frequencies

Radio frequencies as low as 400 KHz to microwave frequencies and milli meter wave frequencies are currently being used for therapeutic applications such as cancer diagnostic application, skin cancer detection and cancer therapy. The frequency range that receives the most attention for biological interaction is the microwave frequency spectrum from 300 MHz- 10 GHz [2]. The attractive feature of RF/ microwave frequency is that they are non-ionizing.

Antennas for biomedical applications can be broadly classified into two different types: antennas for diagnostic imaging and antennas for therapeutic applications.

1.1.1. Antennas for diagnostic imaging

Antennas for diagnostic applications are usually placed outside the body as noninvasive applicators or can be placed in direct contact with the body. Diagnostic applications usually include monitoring the physiological movements and measuring and detecting vital signs such as pressure and temperature variation, heartbeat, respiratory rate etc. in the human body. Magnetic resonance imaging (MRI) uses radio frequency and strong magnetic field to create detailed image of internal organs and tissues within the body and offers much distinct advantages when compared to other imaging modalities. Antennas used for sensing applications passes a beam of electromagnetic energy to the desired tissue and the reflected signal from the body is processed to get the information about the target [3]. Microwave tomography supplements current clinical techniques of deep brain tissue imaging and stroke detection. It exploits the principle of dielectric permittivity variation among the different tissue region to reconstruct the image associated with it [4, 5].

1.1.2. Antennas for therapeutic applications

Antennas for therapeutic applications can be classified into antennas for hyperthermia cancer treatment and antennas for ablation treatment. Hyperthermia treatment uses high temperature to selectively kill the tumor cells without causing any damage to the surrounding normal tissue. Poor blood circulation in tumor helps to accumulate heat in the tumor to destroy it. Patch antennas, waveguide antennas and phased arrays have been proved to be effective in hyperthermia treatment [6]-[8]. Antennas for ablation treatment mainly use interstitial antennas to raise the temperatures up to 50-90 ˚C applied for a shorter duration of time. They are mainly used

to treat cardiac arrhythmia or endometrial disorders. Catheter ablation is an invasive procedure used to remove a faulty electrical pathway from the heart of those who are suffering from cardiac arrhythmia. Embedded antennas are usually used for ablative treatment, where they are inserted through flexible catheters into the blood vessels [9]. The performance of these antennas involves solving Maxwell's equation together with bioheat equation considering the effect of the electromagnetic source and the target tissue to be treated.

1.2. Motivation

According to the studies conducted by American Cancer Society, cancer is considered as the second leading cause of death in United States [10]. Surgery, chemotherapy or radiation therapy are used for the treatment for cancer. Hyperthermia has been proved to enhance the effects of chemotherapy and radiotherapy without causing any side effects. Many clinical trials in a variety of tumor types show the potential of hyperthermia to improve both local tumor control and survival after radiation therapy [11, 12]. Hyperthermia can be applied to a local region, a specific part of the body or the entire body. The purpose of hyperthermia is to elevate tumor temperatures to the order of 42- 45˚C.

Two major problems associated with hyperthermia are supplying uniform heating over the entire target volume and heating a deeply located tumor in a controlled and localized manner. It should be ensured that whole of the cancerous tissue reaches the desired therapeutic temperature and is destroyed. Also, when treating deep tumors, other nearby healthy tissue regions should not be affected. The effectiveness of treatment depends on the type and size of the applicator, duration of treatment, frequency of applied energy and dielectric permittivity of the tissue to be treated.

The aim of this research is to investigate the use of hyperthermia for breast cancer treatment. A near field focused antenna array was designed and the electromagnetic energy from the antenna array was used to produce a small focused spot sufficient enough to treat a stage I breast cancer without causing any damage to the surrounding healthy breast tissue. The antenna array to be used for the treatment is compact and can be used non-invasively without causing any discomfort to the patient.

1.3. Dissertation outline

This dissertation consists of 7 major sections. The first chapter is an outline of the applications of radio frequency/microwave frequency in medicine. It presents an overview of hyperthermia treatment method for cancer and the motivation behind this research.

Chapter 2 covers the biological and electromagnetic characteristics of hyperthermia. This chapter deals with the propagation of electromagnetic waves in biological tissues and the changes in the wave property with the electrical parameters of human body.

Chapter 3 deals with the different type of hyperthermia applicators and their properties. It also explains the process by which the different applicators achieve the required temperature needed for hyperthermia. This chapter also covers the heat transfer process in microwave hyperthermia using the Penne's bioheat equation.

Chapter 4 introduces the grid antenna array proposed for hyperthermia treatment. The advantages of grid antenna array for this application are explained and the effect of applicator on a breast and tumor model is studied.

Chapter 5 proposes a near field focused antenna array for hyperthermia treatment. The antenna array was used to treat a spherical tumor in a hemi-spherical breast tissue and the results for power density, specific absorption rate and temperature increase are presented.

Chapter 6 outlines the conclusion of this dissertation.

CHAPTER 2: BIOLOGICAL AND ELECTROMAGNETIC ASPECTS OF HYPERTHERMIA

2.1. Biological effects of microwave frequencies

The biological effects of microwave frequencies depend on the dielectric fields inside the body. The intensity of electric fields inside the body is determined by the frequency of the applied field, polarization, size, shape and dielectric properties of the body [13]. The depth to which microwaves can penetrate the body is a function of the electric and magnetic properties of the body and the frequency of the applied microwave power. At lower frequency, the depth of penetration is more due to skin effect. For a given frequency, the depth of penetration is inversely proportional to the water content in the tissue. Lower the water content in the tissue, deeper will be the depth of penetration.

When electromagnetic waves travel from one medium to another, boundary conditions need to be satisfied at the interface of two different materials. These conditions determine the behavior of the wave interactions in biological system. Biological materials are lossy and hence power will be deposited in the lossy material as the wave propagates through it. If power is deposited in the material, the material will heat up and this is the basic principle used in hyperthermia application.

2.2. Electromagnetic wave propagation

The human body is an inhomogeneous lossy dielectric material. This lossy nature affects the way in which the electromagnetic wave propagates through human body. As the wave propagates through the body, power will be deposited in the body allowing it to heat up. This

property allows RF/ microwave frequency to be used for hyperthermia application which will be described in detail in a later chapter.

In a lossy biological material as the wave propagates through the tissue, its magnitude decreases exponentially. A propagating electromagnetic wave along z direction is of the form

$$\overrightarrow{E(z)} = E(0).e^{-\alpha z}.\sin(\omega t - \beta z)\,\hat{z} \tag{1}$$

where α represents the attenuation constant and β is the propagation constant in the medium. E (0) is the incident field at the surface of the body and z is the distance the field penetrated the body.

The attenuation constant denotes the rate at which the wave attenuates as it propagates through the medium. It is a function of permittivity and conductivity of the material and the frequency of the electromagnetic wave. The attenuation constant is given by

$$\alpha = \omega \sqrt{\frac{\mu'\varepsilon'}{2}\left(\sqrt{1 + \left(\frac{\sigma_{eff}}{\omega\varepsilon'}\right)^2} - 1\right)} \tag{2}$$

where σ_eff is the effective conductivity, ω is the frequency of the propagating electromagnetic wave, μ′ and ε′ represents the real part of complex permittivity and permeability of the material. Biomaterials are non-magnetic and hence $\mu' = \mu_0$. From equation (2), it is seen that the attenuation increases with increase in conductivity and frequency.

The propagation constant denotes the amount of phase shift a propagating wave undergoes as it propagates through the medium. This constant is also a function of permittivity, conductivity and frequency. The propagation constant is given by

7

$$\beta = \omega \sqrt{\frac{\mu'\varepsilon'}{2} \left(\sqrt{1 + \left(\frac{\sigma_{eff}}{\omega\varepsilon'}\right)^2} + 1 \right)} \qquad (3)$$

The attenuation, α is used to determine an important parameter called skin depth. Skin depth is defined as the distance within the material that the wave propagates before its magnitude has dropped to about 37 % of its original value. The skin depth is given by

$$\delta = \frac{1}{\sqrt{\omega\mu\sigma/2}} \qquad (4)$$

where σ is the conductivity, ω is the frequency of the propagating electromagnetic wave and μ represents the permeability of the material. The skin depth decreases when the frequency increases and is inversely proportional to the square root of frequency and the conductivity. This implies that, when high frequency microwaves are used for medical application, the smaller will be the depth of penetration. When a human body is subjected to a microwave field, the internal organs are not affected if higher frequencies are used.

2.3. Layered body model and wave propagation

The electrical properties of human body are described in terms of permittivity and conductivity. These properties of biological tissue are mainly determined by the water content in the tissue. Biological tissue can be classified as tissues with low water content and high-water content [14]. Low water content tissues have comparatively low permittivity and conductivity, which leads to reduced attenuation, when penetrated by an applied electromagnetic wave [15]. Fat or breast tissue, bone and inflated lungs are all examples of low water content tissue. Skin and muscle are examples of high-water content tissue.

8

To characterize the wave propagation and absorption of electromagnetic field inside human body, a simple three-layer tissue model as shown in Figure 1 is used for basic analysis. Electromagnetic fields can be transmitted from the exterior to the interior of the body through the different layers of the body. Each layer has a permittivity and conductivity which are frequency dependent. The typical thicknesses of the layers are given in [16]. The field will be attenuated by the lossy tissues and reflections occur within the layers. Required boundary conditions need to be satisfied at the interface between the layers. The absorbed fields in the fat layer will be much larger than the field in the skin and muscle layer due to the low permittivity of the fat layer. These higher field concentrations heat up the fat layer producing surface heating.
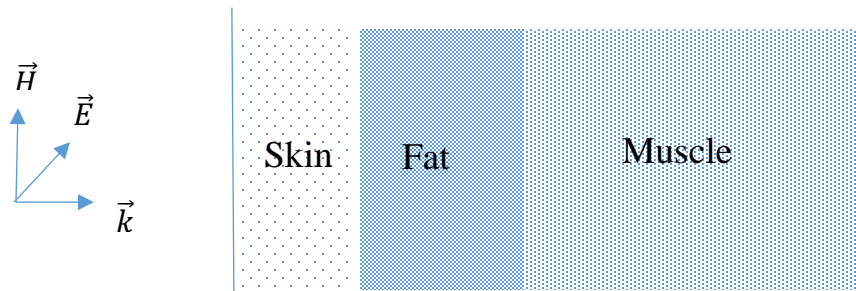
Figure 1: Layered planar tissue model

Table I presents the permittivity and conductivity of some of the body tissues at 900 MHz, 1.8 GHz and 2.45 GHz [16]-[18].

Table 1. Dielectric properties of body tissues

Tissue type	900 MHz		1800 MHz		2450 MHz	
	Permittivity	Conductivity (S/m)	Permittivity	Conductivity (S/m)	Permittivity	Conductivity (S/m)
Skin	41.4	0.87	38.9	1.18	38	1.46
Fat	5.42	0.05	5.27	0.09	5.15	0.14
Muscle	55	0.94	53.6	1.34	52.7	1.74
Bone	12.5	0.14	11.8	0.28	11.4	0.39
Breast	5.42	0.049	5.27	0.09	5.15	0.14
Heart	59.9	1.23	56.3	1.77	54.8	2.26
Lungs	36.7	0.66	35.2	0.96	34.4	1.24
Liver	46.8	0.85	44.2	1.29	43.0	1.69
Kidney	58.7	1.39	54.4	1.95	52.7	2.43

When a propagating electromagnetic wave travels from one medium to another, the waves can get reflected, transmitted or absorbed depending on tissue conductivity, permittivity and the frequency of the source. The waves undergoing reflections at the tissue layer interface can create standing waves and increased energy absorption in some of the layers based on the permittivity and conductivity of the layers. This absorbed energy is converted into heat. Energy absorbed will be high in tissues with high water content than in tissues with low water content.

2.4. Energy absorption

As the electromagnetic wave propagates through a biological medium energy is absorbed by the medium as discussed above. This absorbed energy is quantified in terms of specific absorption rate or SAR. SAR is directly proportional to the effective conductivity of the tissue. Specific absorption rate is defined as the rate at which energy is absorbed by the body when exposed to electromagnetic fields. It is defined as transferred power divided by mass of the object.

$$SAR = \frac{\sigma_{eff}E_{rms}^2}{\rho} \text{ W/Kg} \tag{5}$$

where ρ denotes the mass density of the object and E_{rms} is the rms value of the electric field and σ_{eff} is the effective conductivity.

SAR tells us how much energy is absorbed by the body, when an electromagnetic wave is incident on the body tissue. Different permittivity and conductivity of the various tissues of the body make the SAR values vary throughout the body. Several methods of SAR determination are based on thermal measurements, when a tissue is exposed to RF or microwave energy. The rate of temperature change in the tissue exposed to microwave energy is related to SAR as

$$\frac{\Delta T}{\Delta t} = \frac{SAR}{C} \tag{6}$$

where ΔT is the temperature increase, Δt is the duration of exposure and C is the specific heat.

The thermal effects resulting from the absorption of electromagnetic waves inside biological tissue is described in terms of bioheat equation. The levels of SAR influences thermal effects. One W/Kg of SAR generates an increase of 1℃ in the human body.

Even though electromagnetic energy provides several benefits, it also constitutes hazards to individuals through uncontrolled and excessive emissions. A limit needs to be set on the amount of exposure that individuals can accept safely, and these limits are frequency dependent. At higher frequencies, the depth of penetration is less, radiation is limited to superficial tissue layers. The limits of energy absorbed is usually defined in terms of 1 or 10 g of tissue. Guidelines for limiting electromagnetic exposure provide protection against adverse health effects.

In conclusion the electrical properties of tissue such as permittivity and conductivity control the behavior of propagation in tissues. Choice of antenna types for biomedical application considers factors such as frequency of operation, time duration of exposure, the type of tissue that needs to be treated etc. The medical devices using microwaves depend mainly on the ability of microwaves to penetrate deeply into the living tissue.

CHAPTER 3: OVERVIEW OF HYPERTHERMIA

3.1. Hyperthermia

Hyperthermia is a therapeutic procedure used for the treatment of some case of cancer. It is used to raise the tumor temperature to a higher value than the surrounding normal body tissues to destroy the cancerous cell. It involves achieving and maintaining temperatures of the order of 42-45 ˚C for several minutes at the tumor location. A higher level of water content present in tumor cells increases its conductivity leading to higher absorption of electromagnetic energy. The use of heat to destroy tumors dates back to hundreds of years. In addition to killing the tumor cells, hyperthermia treatment has also been shown to increase the effectiveness of chemotherapy and radiotherapy [19].

Heat is generated, when electric dipoles in the tissue oscillate in response to an applied electric field, generated by the applied electromagnetic energy. This heating is proportional to the permittivity and conductivity of the tissue. As the frequency of electromagnetic wave increases, the wave will not penetrate to an appreciable depth and hence heating cannot be achieved in deeper region of the tissue. For lower frequency applications, field can penetrate well into the body with little control and spread widely. A trade-off between penetration and focusing, low and high frequencies and controlling the power within the body needs to be considered when selecting applicators for hyperthermia for cancer therapy.

Hyperthermia can be performed on the whole body, or be regional or localized, depending on the size of the tissue region to be heated. In whole body hyperthermia, the entire body temperature is raised to 42 ˚C, which may be uncomfortable for the patient and tumors may not

reach the required temperature. Regional hyperthermia heats moderately large volumes including the cancerous region and the surrounding healthy tissue. In localized hyperthermia, only the local tumor region is heated and is mainly used for the treatment of surface tumors.

Two most important challenges associated with hyperthermia for cancer treatment, are providing uniform heating of the entire target volume to ensure that all the tumorous tissue reach the required temperature to destroy it and at the same time not overheat the surrounding healthy tissue region. Quality of hyperthermia treatment depends on achieving higher tumor temperatures and treatment planning. Clinical applications of hyperthermia treatment planning are proper selection of applicator, analysis of heating ability and online treatment guidance. Ongoing developments of treatment planning focus on dielectric imaging, advanced thermal modelling and biological modelling to predict the radiation effect in terms of equivalent radiation dose needed [20].

3.2. Hyperthermia applicators

Hyperthermia applicators can be broadly classified into noninvasive and invasive applicators. Non-invasive applicators use external devices to produce the electric field, while invasive applicators penetrate the body through skin or other natural body opening.

Based on the mechanism used for heating, they can be classified as capacitive applicators, inductive applicators and radiative applicators. Each of these will be discussed in the next section.

3.2.1. Capacitive applicator

These applicators are normally used for deep heating and the applied frequency is relatively low. An example of this type of applicator is presented in [21]. Here RF current flow is produced

by a pair of capacitively coupled electrodes and heating is achieved in the center portion of the phantom without causing any superficial heating. The advantage of capacitive applicator is its simplicity and the ability of the electrodes to curve to match the skin's contour. A common disadvantage of these type of applicator is that they burn the superficial areas of the body when try to heat the deeper tissue. To reduce the risk of skin burn, a water bolus can be placed between the electrodes and the tissue region.

3.2.2. Inductive applicator

An inductive applicator uses an external coil to produce a magnetic field inside the body. The magnetic field by itself will produce no heating, but when there is a time variation of magnetic field, it will induce an internal electric field for heating. These applicators are designed to operate at low to moderate frequencies and typically operate at frequencies of the order of 13 to 27 MHz. Since they are operating at a low frequency, they are mainly used for deep tumor heating. One of the major disadvantages of inductive applicator is that the E field pattern is not optimum for deep heating of the tissue. The heating pattern has a parabolic shape. Surface heating is another important problem associated with inductive applicators. In [22] a heat focusing method onto a deeper portion of the phantom using a pair of inductive aperture type applicator is well explained.

3.2.3. Radiative applicators

These types of applicators rely on the coupling of electric field and magnetic field to deposit electromagnetic energy into the tissue for both surface heating and deep tissue heating. When localized surface heating is needed, they operate at higher frequencies and for deeper penetration they operate at lower frequencies. They use either a waveguide applicator or a patch antenna applicator. For heating large tissue volumes, low frequency radiators are used. Deep body

15

heating is achieved with an array of antennas to focus the heat energy to the desired tumor region. At low frequencies the penetration depth is less, and the applicator becomes bulky. Localized heating is hard to achieve at low frequency. No localization of heat at deeper tissue regions is possible with these types of applicators.

3.2.4. Invasive applicators

To obtain localized heating pattern at deeper tissue regions, invasive applicators are used. They can be inserted using flexible catheters into the blood vessels or directly through skin. They usually use a single antenna or one or more antennas around the tumor region. In [23], a floating sleeve coaxial dipole antenna is used to achieve localized SAR pattern for hepatic microwave ablation. The advantage of the interstitial applicator is that localized heating can be achieved in a smaller volume at greater depths.

3.3. Antenna array applicators for hyperthermia

A literature review of antenna arrays used for hyperthermia treatment and operating in the near field region was done and is summarized in Table 1. The Table shows their frequency of operation, the type and size of the array and the targeted tissue region. In addition, it shows whether any matching medium was used with the applicator to provide impedance matching and how far the applicator was positioned from the tissue. In each case the type of result considered are shown.

Table 2. Antenna arrays reported for hyperthermia operating in the near field region

Freq.	Tissue type	Size	Array	Position from tissue	Matching medium	Results presented
915 MHz [24]	Breast	15 cm cylindrical cavity	Tapered microstrip patch (12 element array)	Breast in prone position 7.5 cm	Water bolus	Power distribution
915 MHz [25]	Arm	17 cm dipole antenna	8 dipoles in circular array of diameter 22 cm	2 cm	Water bolus	E-field distribution
433 MHz [26]	Homogeneous Fat	Microstrip Patch (56 cm x 50 cm)	4 x 2 planar array	174 mm	Water bolus	SAR distribution
915 MHZ [27]	Breast	Waveguide (size not reported)	2 waveguide arrays	2 -3 mm from patient skin	No	E-field pattern

434 MHz [28]	Four-layer tissue	13cmx 13cm	Single patch	2.7 mm	Water bolus	SAR distribution

A similar survey was conducted for antenna arrays operating in the far field region and is summarized in Table 2. The Table summarizes the frequency of operation of the array, the type of array used and its size and the tissue region that was targeted. In addition, it shows whether any matching medium was used with the applicator for impedance matching and how far the applicator was positioned from the tissue. In each case the type of result considered are also shown.

Table 3. Antenna arrays reported for hyperthermia operating in the far field region

Frequency	Tissue type	Size	Array	Position from tissue	Matching medium	Results Presented
2.45 GHz [29]	Muscle	20 mm x 14 mm	4 horn antennas	89 mm	Water bolus	Power pattern
4.2 GHz [30]	Breast	45mm x 45mm	4 sub arrays (3 tapered slot antennas)	80 mm	No	Radiation pattern & SAR
433 MHz [31]	Head and neck	28.7 mm x 8 mm patch	12 (2rings of 6 each)	40 mm	Water bolus	E-field
4.86 GHz [32]	Breast	150 mm x 175 mm	Grid array	60 mm	No	Radiation pattern

3.4. Thermal effects of hyperthermia

In biological tissue, the absorption of electromagnetic energy produces an increase in its temperature. The thermal effects due to the exposure to electromagnetic energy is described in terms of Penne's bioheat transfer equation. The equation describes the magnitude of heat transfer between tissue and blood and is used to solve the temperature distribution for thermal therapy [33]. The bioheat equation gives the relationship between time rate of heat accumulated per unit volume at a point inside the body and the corresponding time rate of temperature increase.

3.4.1. Penne's bioheat equation

Once the electromagnetic field inside the target tissue is defined, the corresponding temperature increase due to the absorbed electromagnetic field can be described using equation (7) shown below:

$$\rho c \frac{\partial T}{\partial t} = \nabla . (k \nabla T) + \rho_b c_b \, \omega (T_a - T) + q_{met} + Q_{ext} \tag{7}$$

where ρ denotes the tissue density, T is the temperature inside the medium, c denotes the tissue specific heat, k is the tissue thermal conductivity, ω is the blood perfusion rate, ρ_b is the density of blood, c_b is the blood specific heat, T_a is the arterial blood temperature, q_{met} denotes the volumetric heat generation due to the basal metabolism and Q_{ext} denotes the heat generated by the external source, which in this case is the electromagnetic energy absorbed by the tissue. The heat generated by the absorption of electromagnetic energy, Q_{ext} is given by equation (8) as

$$Q_{ext} = \frac{1}{2} \, \sigma \, |E|^2 \tag{8}$$

where σ denotes the conductivity of the tissue and $|E|$ denotes the electric field magnitude produced by the applied electromagnetic wave.

The thermal parameters for most of the body tissues are available in the literature [34]. Tumors have high blood perfusion rate at the surface and low blood perfusion near the center. This low blood perfusion in the tumor center helps in the accumulation of electromagnetic energy in the center, thereby easing the heating process during hyperthermia treatment. The bioheat equation is used to predict the temperature rise and helps in ensuring that safety standards are met.

3.5. Electromagnetic Regulations

Allowable guidelines and regulations for electromagnetic field exposure are based on the amount of applied electromagnetic power produced from different electromagnetic exposure conditions. There are regulations on allowable frequency, allowable absorbed power in the body, localized exposure limits etc [35].

Allowable frequencies for medical applications cover ISM (Industrial, Scientific and Medical) bands and MICS (Medical implant communication services). ISM bands mainly include 433 MHZ, 915 MHz and 2.45 GHz which are used in external body applications in hyperthermia treatment, cardiac ablation etc. MICS is allocated for implantable devices that will stay in the body for a period of time.

The absorbed power limitation is defined by the specific absorption rate in the tissue. As per the guidelines set by IEEE-ANSI C95.1 standard, a whole body averaged SAR of 0.4 W/Kg is recommended for occupational situations and a value of 0.08 W/Kg for general public [36]-[37]. A limit was set by IEEE-ANSI C95.1 for the localized SAR as 1-g SAR exposure limit of 1.6 W/Kg for uncontrolled exposure and 2 W/Kg for controlled exposure.

CHAPTER 4: GRID ANTENNA ARRAY FOR HYPERTHERMIA TREATMENT

4.1. Introduction

In this chapter a microstrip grid antenna array is introduced for hyperthermia treatment of breast cancer. This method presents a non-invasive way of cancer treatment to raise the temperature of the tumor to levels sufficient enough to destroy it. Electromagnetic and thermal simulations were performed on a cubical model of the breast tissue and the results are presented. The electromagnetic energy absorption in the breast tissue was studied in terms of specific absorption rate (SAR) inside the tissue. The SAR values inside the breast tissue and the tumor tissue were plotted and the extent of heating zone was studied by plotting the temperature profile with tumor located at the center of the breast tissue. The array is positioned such that the maximum power density location coincides with the center of the tumor tissue. The antenna array was able to raise the temperature of the tumor to around 44 ˚C in a short amount of time.

4.2. Grid antenna Array: Literature review

A grid antenna array is a planar, low profile antenna array which was first introduced by Kraus in 1964 [38]. Kraus proposed this array as a linearly polarized, travelling wave, non-resonant antenna array. Its initial design consisted of grid or mesh array placed parallel and close to a conducting sheet which acts as the ground plane. Conti et al. reported the first microstrip version of grid array and the array was a linearly polarized resonant antenna [39]. The major advantages of the grid antenna array are its high gain, narrow beam, simple feed, broad bandwidth and low side lobe levels [40, 41].

Different variations of the grid antenna array and its basic theory and applications are well explained in [42]. According to their studies the array finds wide application from low microwave frequencies to millimeter wave frequencies. The basic structure of grid antenna array consists of rectangular meshes of microstrip lines on a dielectric substrate with a conducting ground plane behind the substrate. The array can be fed using a coaxial cable in the center of the array or at one of the edges of the array with the other edge terminated. The array can work as a resonant or non-resonant antenna based on the electrical length of the edges of the mesh. For a resonant grid array antenna, the longer side will be one wavelength and the shorter side will be one half wavelength in the dielectric. This produces an in-phase current on the shorter side and out of phase current on the longer side resulting in a main lobe beam of radiation in the bore sight direction. For a non-resonant grid array antenna, the shorter side of the rectangular mesh is slightly greater than one third of wavelength and the length of the longer side of the mesh is more than two times the shorter side and less than three times the shorter side of the mesh. When a non-resonant grid array is fed from one end, the current in the shorter side of the mesh will follow a phase progression resulting in main lobe beam of radiation in the end fire direction. Thus, in short, for a resonant grid array antenna, the shorter side of each rectangular mesh acts as the radiating element and the longer side mainly acts as transmission lines.

When the grid array operates as a travelling wave non-resonant antenna, there is no precise beam control or no scanning beam at a specific frequency. So, a grid antenna array is more popular as a non-travelling wave resonant antenna, where the antenna is fed in the center and the array produces a fixed beam in the boresight direction.

4.3. Proposed grid antenna array for hyperthermia

In applications for hyperthermia, the antenna array is designed such that it can be placed around the region that needs to be radiated. For example, as a circular ring around the torso, head and neck, breast etc. Using an array of applicators for hyperthermia provide greater penetration depths. Array applicators also provide means for obtaining a narrow radiation beam with high gain and better focusing of the radiation on the cancerous tumor. The phase of each individual element of the array needs to be adjusted to focus heat onto the desired tissue region. This often requires a complex feeding network. In order to overcome this limitation, the use of a compact wide band grid antenna array is proposed. As discussed earlier, the array can be fed at the mesh cell center or at the mesh cell edge with other edge terminated. The antenna is fed by a metal via through an aperture on the ground plane using a coaxial cable. The applicator can be placed on a rotating arm allowing it to be moved near to the location of the tumor. Here we are proposing a wide band and compact microstrip antenna array for hyperthermia treatment of breast cancer.

In [43] a grid antenna array was proposed for hyperthermia breast cancer treatment system. The conventional grid array antenna was modified in their study to get suitable radiation properties needed for hyperthermia applications. Both electromagnetic and thermal simulation results were presented, and a comparison of the conventional grid array and modified grid array is also presented. The antenna array was designed for 4.86 GHz and was able to produce a temperature increase of 8°C in breast phantom in 10 minutes with 0.5 W input power. Their design raised the temperature of entire breast tissue to 46 °C, irrespective of tumor or normal healthy tissue. So, the procedure presents the danger of damaging the healthy breast tissue also. Here a

24

modified design is presented to raise the temperature of a tumor that is located in the center of the breast without heating the surrounding healthy tissue.

4.3.1. Antenna Design

The proposed grid antenna array applicator along with its dimensions is shown in Figure 2.
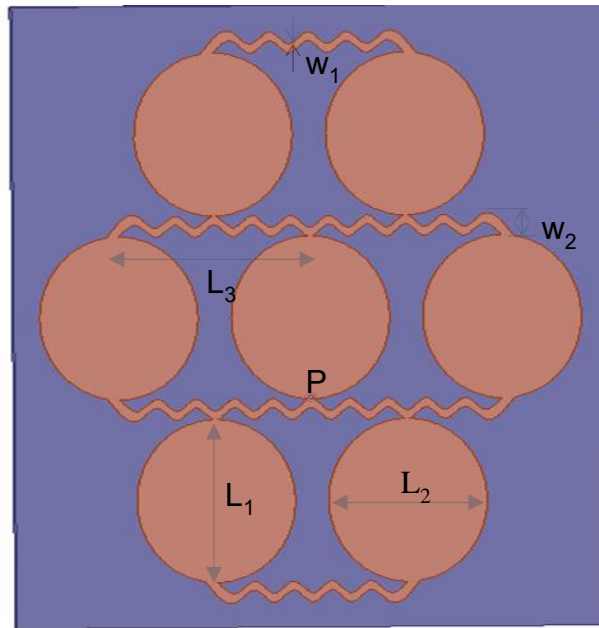
Figure 2: Grid array applicator with L_1 = 65.6 mm, L_2 = 45.5 mm, L_3 = 55 mm, w_1= 3.6 mm and w_2 = 8.4 mm

This design was adopted from [44] as it was compact and had a high frequency bandwidth. For applications in hyperthermia, we need an antenna that is compact, has high gain and simple feed and this array meets these requirements. The array consists of two types of grid cells of which one of them acts as the radiation element and the second one functions as a transmission line. Here the radiation elements are elliptical, and the transmission lines are sinusoidal. The elliptical radiation elements provide a more compact design and the sinusoidal transmission lines between the elements allow for achieving a larger frequency bandwidth.

The antenna is designed to operate at a frequency of 2.45 GHz, which is one of the typical frequencies used for hyperthermia application in the ISM band. The array uses a dielectric substrate with $\varepsilon_r = 2.65$ with a thickness of 1 mm. The overall size of the grid array applicator is 170 x 250 x 1 mm^3. A metal reflector is placed at the back of the substrate at a distance of 6.42 mm, which acts as the conducting ground plane and also provides gain enhancement. Its size is set to 10 mm larger than grid array size in both X and Y directions. The space between the substrate and the metal reflector is filled with air. The antenna array is center fed directly at point P, with a 50 Ω coaxial line. The antenna array is linearly polarized.

4.3.2. Return loss and power density

The performance of the antenna array was simulated in HFSS. The radii of the ellipse, length of the sinusoidal transmission line and the location of the feed point was adjusted to get a resonant frequency of 2.45 GHz. Fig. 3 shows the reflection coefficient variation of the patch array in free space and when placed in front of the breast tissue. As can be seen from the figure, the array is well matched with a return loss less than -10 dB at the frequency of 2.45 GHz.
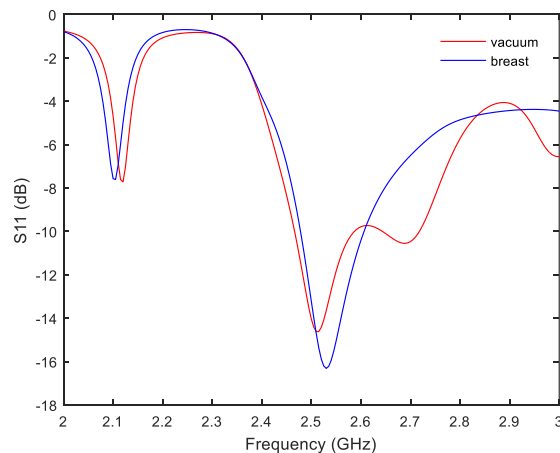
Figure 3: Return loss performance of the antenna array
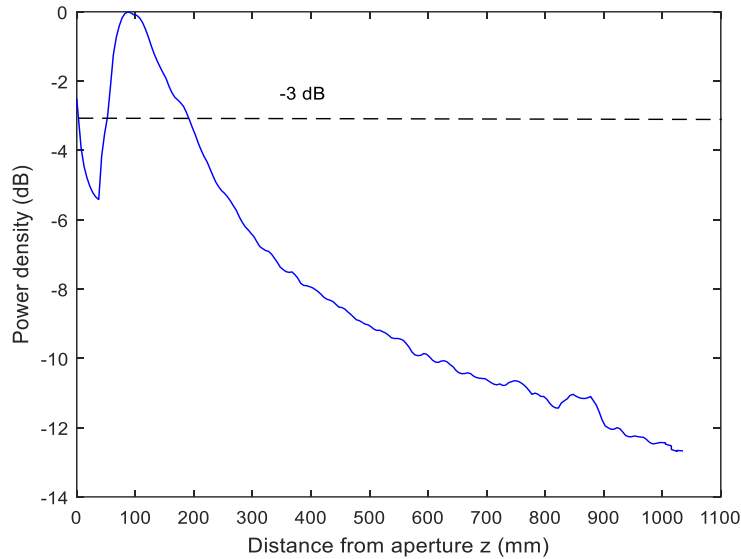
Figure 4: Normalized power density along Z direction

With antenna placed in free space, the normalized power density along the Z direction from the antenna aperture was plotted and is shown in Figure 4. It can be seen that in free space the power density is maximum at a distance of 87 mm from the antenna aperture. The depth of focus, which is defined as the distance between the two -3 dB points on either side of the maximum power density, is found to be 140 mm. In order to find the width of the -3 dB spot area, a contour plot of the power density was plotted at the location of maximum power density at Z=87 mm and is shown in Figure 5. The width of -3dB spot is found to be 60 mm x 80 mm in the X-Y plane. The width of this region is very important in medical applications as this is the region where the electromagnetic energy is mostly concentrated. Antenna array used for hyperthermia application needs to produce a focal spot that is sufficient enough to cover the entire diseased tissue region without affecting the healthy tissue region.

27
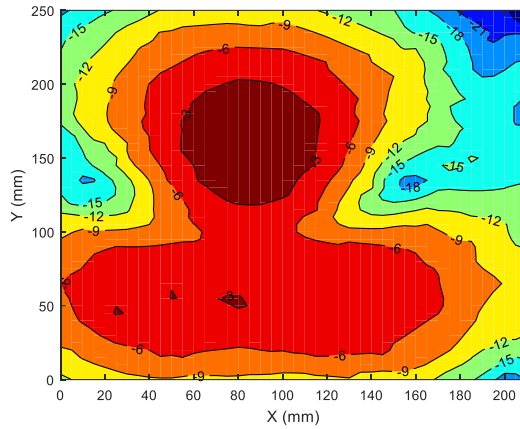
Figure 5: Contour plot of normalized power density at a distance of 87 mm from antenna aperture

4.3.3. Results with breast model in front of applicator

A cubic model of the breast was considered for this study. The breast tissue model with a depth of 10 cm along Z direction was considered and the X and Y dimensions of the breast tissue model was taken the same as the X and Y dimensions of the antenna array. The permittivity and conductivity of the breast tissue used for the simulation at 2.45 GHz are ε_r = 5.14 and σ = 0.13 S/m, respectively [45]. A spherical tumor of diameter 1 cm was used to study Stage 1 cancer treatment in this study and was placed at the center of the breast tissue. The applicator was placed in front of the breast model at a distance of Z=87 mm.

Figure 6 shows the contour plot of normalized power density at a distance of 88mm from the antenna aperture where the power density was maximum. The width of -3 dB spot in this case is found to be 6.5 cm x 6.5 cm, which is less than that in free space and the depth of focus was 110 mm.
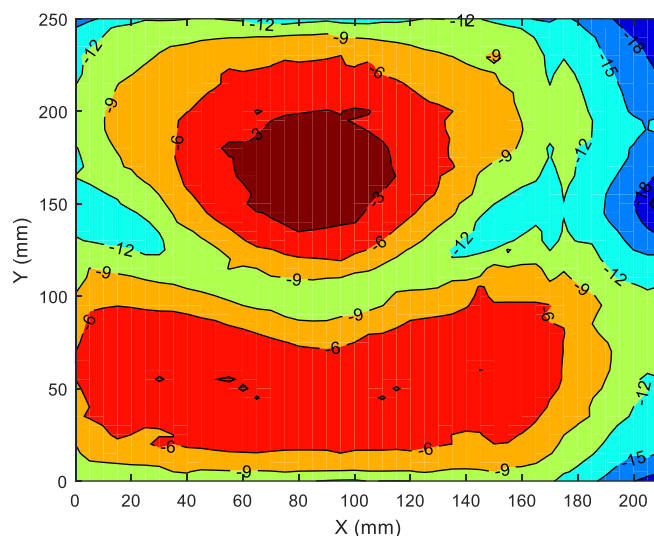
Figure 6: Contour plot of normalized power density at the maximum power density location inside the breast tissue

In order to study the amount of electromagnetic energy absorbed in the breast tissue and the corresponding temperature increase, the specific absorption rate (SAR) inside the tissue was studied. To avoid damage to the healthy tissue, the SAR value must be less than 2W/kg averaged over 10 g of tissue and less than 1.6 W/kg averaged over 1 g of human tissues, as per the guidelines set by the Federal Communications Commission (FCC) and International Commission on Non-Ionizing Radiation Protection (ICNIRP) [46]. Specific absorption rate variation was studied using SIM4LIFE software [47].

The SAR along the depth of the breast tissue was plotted and is shown in Figure 7. The maximum SAR value was 2.97 W/Kg at the center of the tumor tissue at Z=137 mm and for the entire volume of the tumor tissue the SAR value was 3 W/Kg and was greater than 2 W/Kg limit set by the ICNIRP guidelines. For the surrounding healthy breast tissue SAR was less than 2 W/Kg.

29
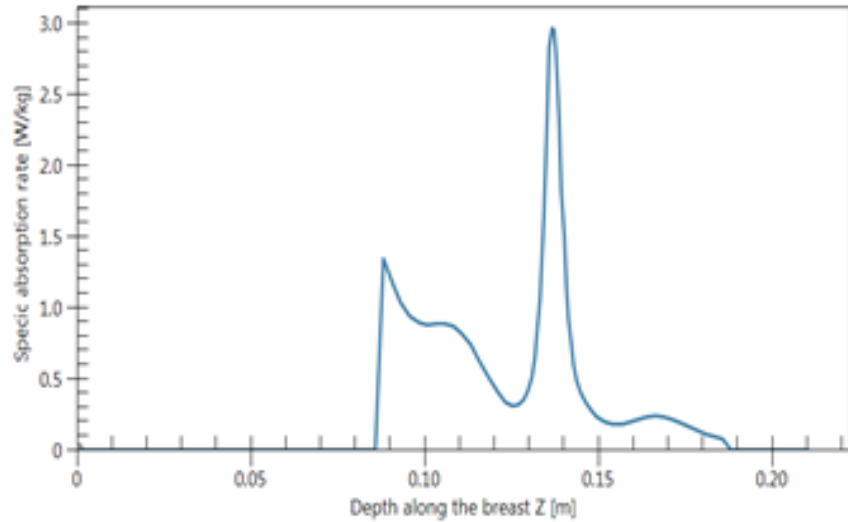
Figure 7: Specific Absorption Rate variation along the depth of the breast tissue

An increase in the specific absorption rate produces a corresponding increase in the temperature and in order to study the temperature variations, thermal simulations were performed using SIM4LIFE software [47]. The thermal properties of breast tissue and tumor tissue used for simulation is shown in Table 4.

Table 4. Thermal properties of breast tissue and tumor tissue at 2.45 GHz

Tissue	Density (kg/m³)	Specific heat (J/kg.K)	Thermal conductivity (W/m.K)	Metabolic heat generation rate (W/Kg)	Perfusion rate (/s)
Breast	911	2348	0.209	0.7279	0.0013
Tumor	1050	3770	0.48	65	0.012

Fig. 8 shows the variation of temperature along the depth of the breast tissue. The maximum temperature of 44.4˚C occurs at the center of the tumor (Z=137 mm) in the middle of X-

Y plane. Temperatures greater than 42˚C suitable for hyperthermia, extend for depths of around 10 mm in the tumor, covering the entire tumor region.
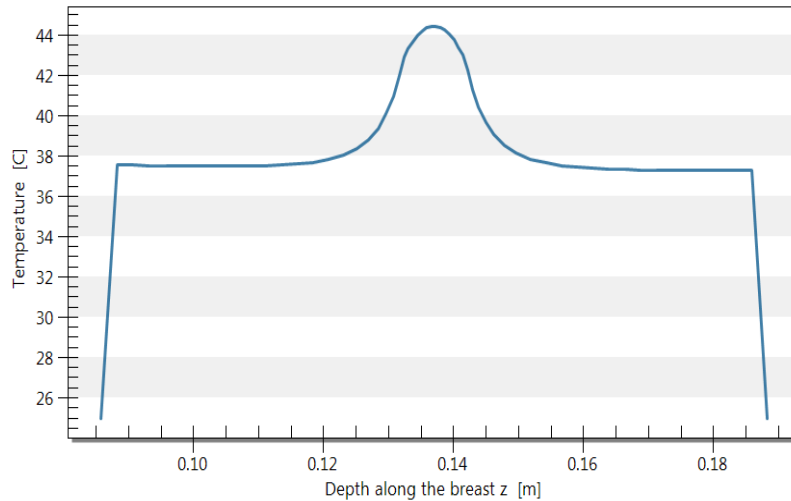
Figure 8: Variation of temperature along the depth of the breast tissue

The temperature profile was plotted at the location of maximum temperature inside the breast tissue. The temperature was maximum at the center of the tumor tissue and the maximum temperature was found to be 44.4 ˚C. Figure 9 shows the temperature profile in the X-Y plane at the location of maximum temperature inside the breast tissue. The region inside the green circle in the temperature profile highlights temperatures greater than 42 ˚C, for the entire tumor volume, which is the required temperature for hyperthermia application.
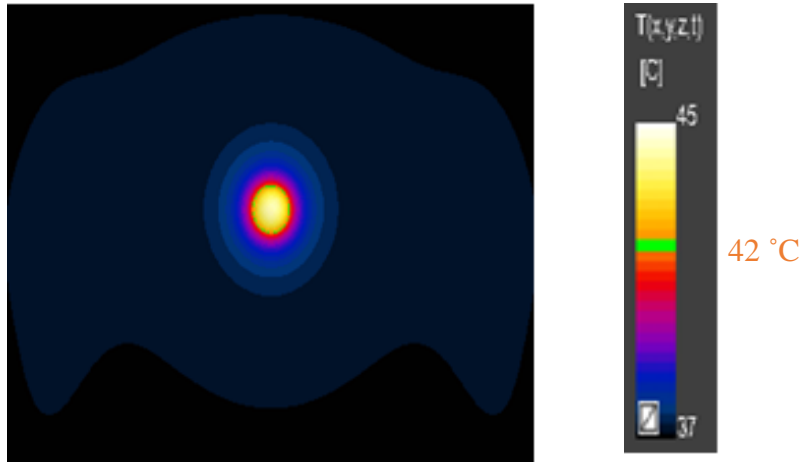
Figure 9: Temperature profile in the breast tissue at the plane of maximum temperature

The transient temperature inside the breast tissue at the location of maximum temperature was plotted and is shown in Figure 10. The temperature increases with time and reaches a maximum value of 44.4 ˚C in almost 10 minutes and thereafter remains at steady state temperature.
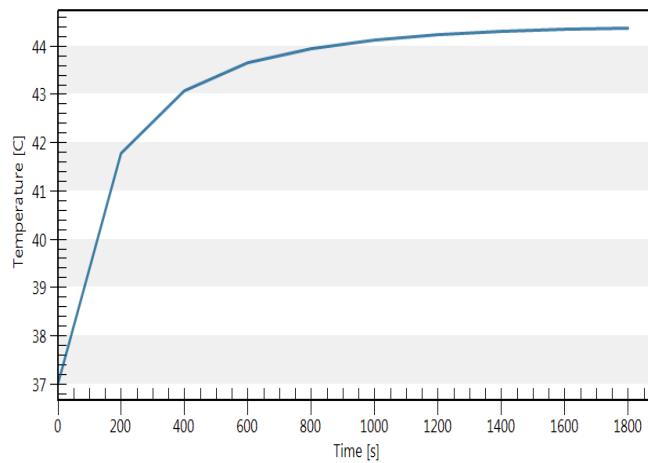
Figure 10: Temperature variation with time at the location of maximum temperature

It has been reported in [48] that there is a 100 % survival rate for tumors smaller than 2 cm, for breast cancer that has not spread to lymph nodes. Based on this we need to have a focused

spot less than 2 cm for Stage I cancer treatment and that can be attained with the proposed grid antenna array.

4.4. Conclusion

In this Chapter, hyperthermia treatment method for breast cancer using a grid array antenna was presented. The grid array antenna presented here was a compact, wide band antenna printed on a dielectric substrate with a metal reflector at the back for gain enhancement. The elliptical radiation elements in the array enhances the impedance bandwidth of the antenna, while the sinusoidal transmission line helps to have a compact design. Another attractive feature of this array was its simple feed, the antenna can be directly fed from a 50 Ω coaxial line.

The antenna array was used for the treatment of a spherical breast tumor located at the center of a cubical model of the breast tissue. The antenna was operated in the near field region and the breast tissue was placed at the location of maximum power density of the antenna in free space. With this position, the power density inside the breast was maximum close to the surface of the breast. The specific absorption rate was analyzed to determine the energy absorbed by the tumor and the surrounding healthy breast tissue region. It was seen that the absorbed energy was maximum inside the tumor region, while in the healthy breast tissue, the SAR value was less than the maximum allowed value of 2 W/Kg. Thermal simulations were performed to study the temperature increase inside the breast tissue due to the absorbed electromagnetic energy. The temperature inside the tumor was raised to 42- 45 ˚C in about 10 minutes, while the temperature in the healthy breast tissue remain at the normal temperature of 37 ˚C.

The main advantage of this method was that it was noninvasive. It was seen that this heating method was sufficient for the treatment of a stage I breast cancer where the diameter of the tumor is less than 2 cm. The entire heating region extended up to a depth of 1 cm.

One of the main drawbacks of this applicator was that there was no control over the depth of focus. In other words, the location of the focal plane cannot be adjusted as the array elements were fed using a single coaxial feed. Also, the power density was maximum close to the surface of the breast which may cause surface heating of the breast tissue. In order to overcome these limitations and to have a better control over the focus, a near field focused antenna array was proposed. In a near field focused array the phase of excitation of each individual antenna array element can be adjusted to achieve better focusing.

CHAPTER 5: NEAR FIELD FOCUSED ANTENNA ARRAY FOR HYPERTHERMIA TREATMENT

5.1. Introduction

In this chapter a near field focused planar microstrip antenna array is designed and is proposed as an applicator for hyperthermia treatment of breast cancer. A 4x4 planar microstrip antenna array is designed for a frequency of 2.45 GHz which is one of the commonly used frequencies for hyperthermia application. The focusing properties of the array were studied on a spherical tumor located inside a hemi-spherical breast tissue. The proposed antenna array was able to produce a focused region around the tumor tissue. The array was placed at different location around the breast phantom and the specific absorption results were studied. The array was able to produce a small focused spot of the size of a typical Stage I breast tumor. Different placement locations of the tumor were also considered. Studies were also done on spherical model of the breast tissue. Results for the power density distribution and SAR in the breast are presented.

5.2. Near field focused antennas: Literature review

Focused antennas are mainly used in applications requiring higher power densities in moderate ranges. For near field focused antennas, the focal point is located in the antenna radiative near field region. Due to the field spreading factor, the maximum radiated power density is obtained in the radiative near field region not at the focal point, but it is located at a point between the antenna aperture and the focal point. The focusing can be obtained by implementing a symmetric source-phase tapering, that can compensate for the different distances between each source point on the aperture and the focal point [49]. The power-density peak is placed between

35

the focal point and the antenna's aperture. Near field focusing is done to increase the electromagnetic power density in the radiative near field region close to the antenna aperture. The focusing of the array is achieved by controlling the phases of each individual antenna elements in the array such that each element's field contribution is added up in phase to get the maximum at the focal point. Near field focused antennas can achieve the required power density in a spot region around the focal point with minimum radiation in the far field region where the focusing effect is lost. Near field focused antennas find wide applications in wireless remote identification systems, local hyperthermia and imaging systems, wireless power transfer systems and industrial microwave applications [50].

Near field focused (NFF) antenna arrays can be characterized by three most important parameters which are the depth of focus, focal plane width and the axial and side lobe levels [51]. The depth of focus is defined as the distance between two -3 dB points around the point of maximum power density along the direction normal to the antenna aperture. Focal plane width defines the size of the region around the focal point, in a plane parallel to the antenna aperture, where the normalized value of maximum power density is greater than -3 dB. The size of this region is very important when the near field focused antennas are used to increase the spatial resolution in imaging or inspection systems.

Proper tapering of the amplitude of the excitation of array elements is used to control the level of the secondary lobes around the focal spot region. High level of the secondary lobes may reduce measurement accuracy in noncontact sensing applications or heat healthy tissues in microwave hyperthermia systems [52]. Also, high secondary lobe level may reduce transmission efficiency in wireless power transfer systems, increase the interference with nearby wireless

systems, raise the personnel exposure to radiation hazards, and enlarge the number of false positive readings in RFID systems. Conjugate-phase approach is the commonly used design criteria for NFF antennas, but a number of other optimization techniques have been proposed to reduce the side lobe levels, shaping the antenna near field, and achieving a simultaneous control of the near field and far field radiation pattern .Different technologies and layouts can be used to implement the near field focusing. In [52], near field focused arrays are classified as array of printed patches, dielectric resonator arrays, reflect arrays, transmit arrays, Fresnel zone plate lens antennas, leaky wave antennas and waveguide arrays.

When antennas are used for therapeutic application, the electromagnetic field produced in the nearby surrounding region of antenna is more important than the far field parameters. When a NFF antenna array is to be used for hyperthermia application, the antenna array should be capable of heating the entire tumor volume without damaging the surrounding normal tissue. In [53], gain optimization was done to have the maximum power deposited at a specific region in the near field of the antenna array for hyperthermia application to heat biological tissue. An optimal design procedure based on maximization of power transmission efficiency between two antenna arrays is well explained in [54]. A 4 x 2 focused microstrip patch antenna array was designed to operate on fat mimicking phantom at 433 MHz [55] and the specific absorption results showed that energy was focused on the desired region validating the near field focusing procedure for hyperthermia application. A planar microstrip NFF antenna array working at 2.45 GHz was used in medical applications to produce a small focused spot 10 cm x 10 cm^2 [56].

Based on the literature study, it is seen that near field focused antennas can be effectively used for hyperthermia treatment to produce a high energy focused spot in a diseased tissue region

without causing any damage to the surrounding healthy region. The depth of focus and the focal width needs to be optimized based on the region to be treated and on the size of tumor. In the next section the design of a near field focused antenna array that produces a focused spot of 1.5 cm x 2 cm in breast tissue is presented.

5.3. Proposed near field focused antenna

The proposed antenna array is a microstrip planar antenna array with single patch elements designed to operate at 2.45 Hz [56]. The antenna array is designed to treat a spherical breast tumor 1 cm in diameter located at the center of a spherical model of breast tissue.

5.3.1. Antenna Design (single patch)

To evolve to the 4 x 4 microstrip patch antenna array, a single microstrip patch antenna was designed at a frequency of 2.45 GHz. The patch was designed with FR-4 substrate, $\varepsilon_r = 4.4$, loss tangent 0.02 and with a thickness of 3 mm. The patch is fed using microstrip line feeding as it is easier to match by controlling the inset feed position. The length (L) and width (W) of the patch was designed according to the equations given below [57]:

$$W = \frac{c}{2f_r} \sqrt{\frac{2}{\varepsilon_r + 1}} \tag{9}$$

where c is the velocity of electromagnetic wave in free space. For a dielectric permittivity, ε_r, thickness, h and the resonant frequency, f_r, the effective dielectric permittivity is given by the equation:

$$\varepsilon_{reff} = \frac{\varepsilon_r + 1}{2} + \frac{\varepsilon_r - 1}{2} \left[1 + 12\, \frac{h}{W}\right]^{-1/2} \tag{10}$$

The effective length of the patch is L_{eff} is given by

$$L_{eff} = L + 2\,\Delta L \tag{11}$$

The extension of the length of the patch caused by the fringing effects is approximated by the relation given below [58]:

$$\frac{\Delta L}{h} = 0.412\,\frac{(\varepsilon_{reff}+0.3)(\frac{W}{h}+0.264)}{(\varepsilon_{reff}-0.258)(\frac{W}{h}+0.8)} \tag{12}$$

The resonant frequency, f_r is related to the length (L) of the patch by

$$f_r = \frac{c}{2L\sqrt{\varepsilon_{reff}}} \tag{13}$$

The inset feed distance from the radiating edge, y_0 is calculated using equation (14) as

$$R_{in}(y = y_0) = R_{in}(y = 0)cos^2(\frac{\pi}{L}\,y_0) \tag{14}$$

The optimized dimension of the patch, W= 37.3 mm, L= 28 mm, y_0 = 10 mm at f = 2.45 GHz, obtained using HFSS. The width of the inset feed was calculated using the line calculator function in ADS for a 50 Ω input transmission line. The width of the feed, w_f was found to be 5.8 mm. The length of the feed line was 15mm which includes the length of the inset feed. These dimensions are shown in Figure 11(a). Figure 11 (b) shows the return loss characteristics of the single patch from 1 GHz to 3 GHz, showing that the antenna is well matched at a resonant frequency of 2.44 GHz with a return loss of -22 dB. This single patch is used for the design of a 4 x4 patch near field focused antenna array.
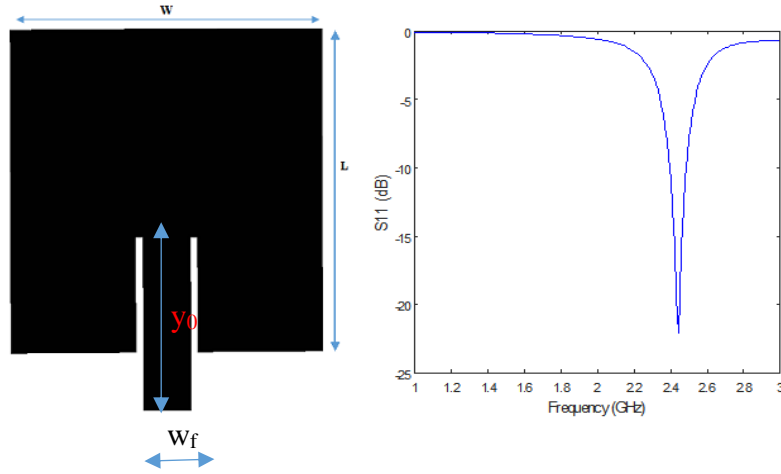
Figure 11: (a) Single rectangular microstrip patch element (b) return loss performance of the

patch

5.3.2. Antenna array design procedure

To achieve near field focusing with a 4 x 4 antenna array the phases of each individual patch element needs to be adjusted such that their individual contribution will add in phase at a designated focal point. In other words, in order to attain field focusing proper phase shift needs to be applied to each element to compensate for the phase difference caused due to the distance of each element from the focal point. This phase shift is obtained by choosing the corresponding electrical length for the feed lines for each individual element of the array.

For a rectangular antenna array placed in the x-y plane with Z axis normal to the antenna aperture, the aperture distribution can be represented as

$$f(x,y) = E_0(x,y) \exp \left\{ jk \left(\frac{x^2+y^2}{2F} \right) \right\}$$
(15)

where $E_0(x, y)$ is the electric field amplitude distribution at the aperture at point (x,y), f is the distance along the z direction at which the antenna is focused and k is the wave number [59].

A quadratic phase tapering as represented by equation (16) will bring the focal spot to a distance f from the aperture, with the center of the array as origin with a phase shift of 0˚.

$$\Theta = k \sqrt{x^2 + y^2 + z^2} - f \tag{16}$$

Uniform amplitude excitation was applied to each individual element of the antenna array. The phase shift needed for each individual element was calculated using equation (16) and was correspondingly set for each individual element of the array by changing the feed lengths. The feed network was designed and simulated using ADS by replacing each patch element by a 50 Ω impedance line. The width of 50 Ω line was 5.8 mm. Quarter wave impedance transformers were used at the output of each T-junction for impedance matching. The width of the quarter wave line was 3 mm.
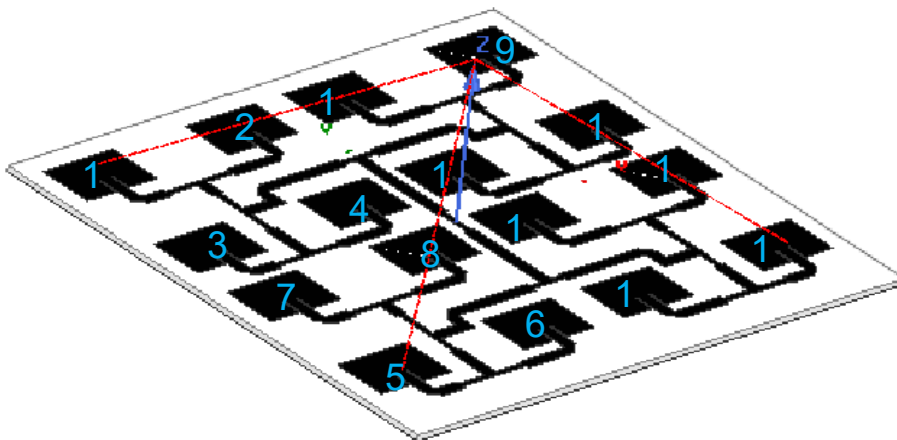
Figure 12: Antenna geometry and quadratic phase distribution

With the center of the 4x4 array chosen as the origin, all the 2 x 2 array elements on all four quadrants of the array are equidistant from the origin. Therefore, the phase distribution of each 2 x 2 sub array on each quadrant will be the same. The patches are separated by 60 mm. The focal distance was set at f = 30 cm along the Z axis from the center of the antenna array. The phase distribution of each element of the array calculated to get this focal point is shown in Table 5.

Table 5. Phase distribution of the patch elements in the array

Array elements	Phase shift
1,5,9,13	138.87
2,6,10,14	78.56
3,7,11,15	78.56
4,8,12,16	16.1

After designing the entire feed network with the required phases, the antenna array was simulated in HFSS. Figure 13 shows the geometry of the 4 x 4 antenna array along with its dimensions. The overall dimension of the 4 x4 array was 260 x 260 x 3mm^3.
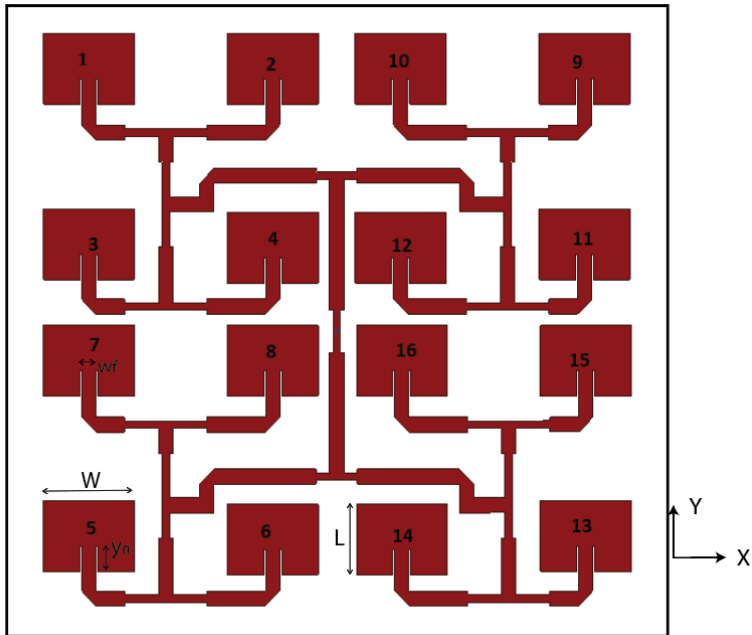
Figure 13: Proposed 4 x 4 microstrip patch antenna array geometry with W= 37.3 mm, L= 28 mm, y_0 = 10 mm, w_f = 5.8 mm

5.3.3. Return loss and power density

Figure 14 shows the return loss performance of the antenna array in free space. The antenna is perfectly matched with a resonant frequency of 2.5 GHz. Figure 15 shows the normalized power density of the antenna array in free space.
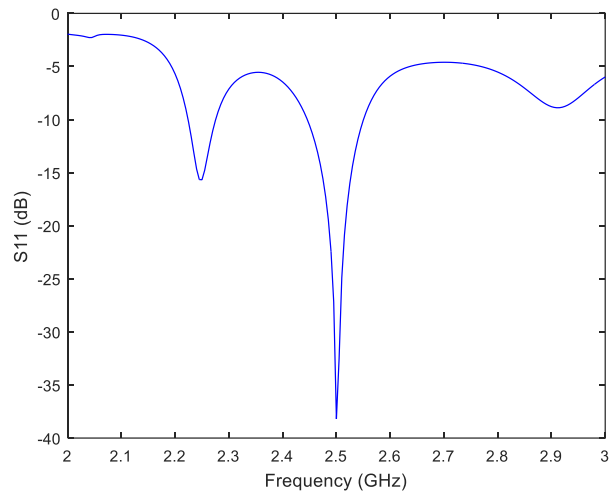
Figure 14: Return loss performance of the 4 x 4 microstrip antenna array
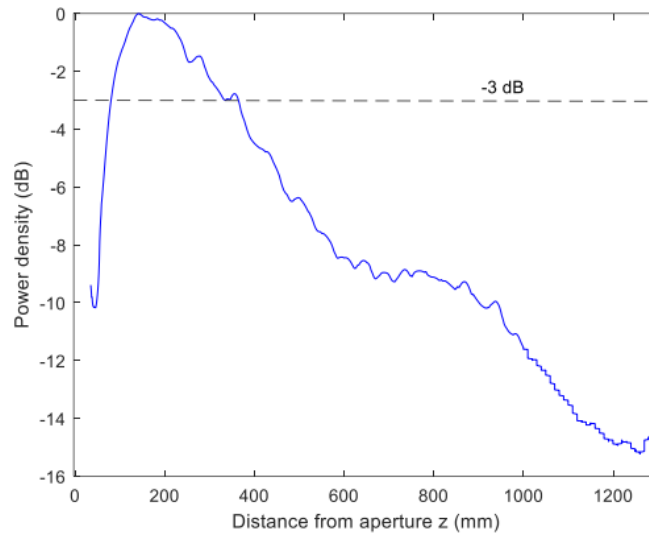
Figure 15: Normalized power density of the antenna array in free space

As can be seen from Figure 15, maximum value of power density occurs at a distance of 130 mm from the antenna aperture. Depth of focus, which is the distance between two -3 dB points on either side of the maximum power density, in free space is 255 mm. This distance tells us the width of -3 dB region along Z direction. A contour plot of the normalized power density in free

44

space at the location of maximum power density (z=130 mm) was plotted and is shown in Figure 16. The width of -3 dB region at the plane of maximum power density was found to be 80 x 110 mm^2 in the x-y plane. This region is very crucial in medical application as this is the region where the concentration of electromagnetic waves is maximum.
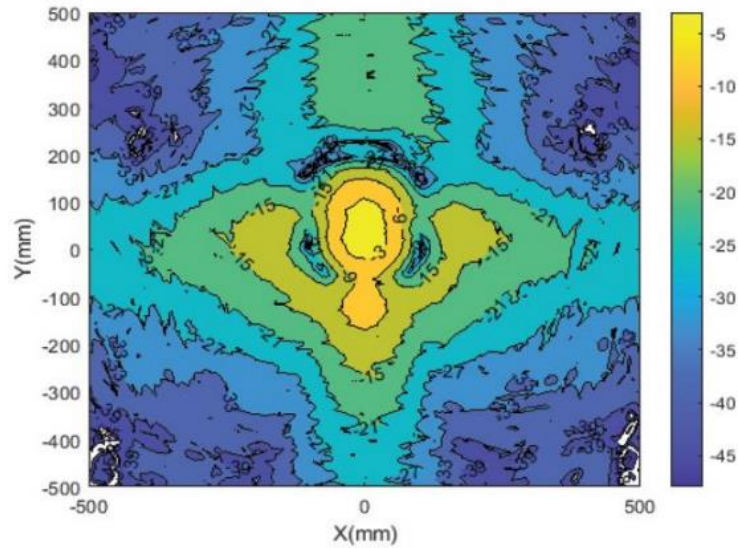
Figure 16: Contour plot of normalized power density at the maximum power density location

5.4. Application of antenna array for breast tumor treatment

The designed 4 x4 microstrip antenna array was able to produce a focused spot at a specific distance of 130 mm from the antenna aperture. The antenna was operated in the near field and for the hyperthermia treatment of a breast tumor. A spherical portion of the breast tissue was analyzed first and then a hemi-spherical breast model was chosen.

5.4.1. Spherical Breast model

For our simulation purpose, we used a two-layer spherical breast model comprising of fat and glandular tissue and a radius of 68 mm. The radius of the fat and glandular region was 5mm

and 63 mm respectively. The electrical properties of fat and glandular tissue are shown in Table 6.

Figure 17 shows the placement of antenna array with reference to the breast tissue.

Table 6. Electrical properties of breast layers

Tissue	Dielectric Permittivity ε_r	Conductivity σ (S/m)
Fat	10.8	0.268
Glandular tissue	27	0.9
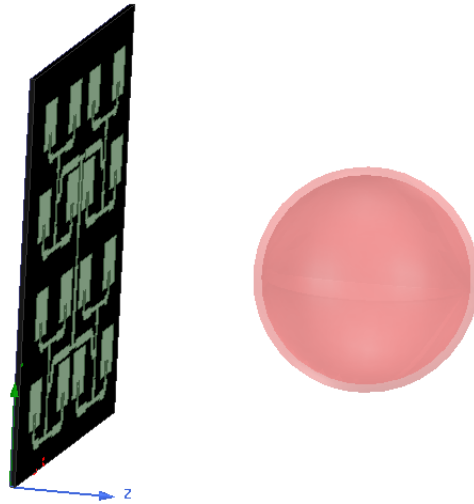
Figure 17: Placement of antenna array and breast tissue

The antenna array is placed at a distance (z=130 mm) such that the center of the breast tissue coincides with the plane of maximum power density in free space and Figure 18 shows the contour plot at this location.
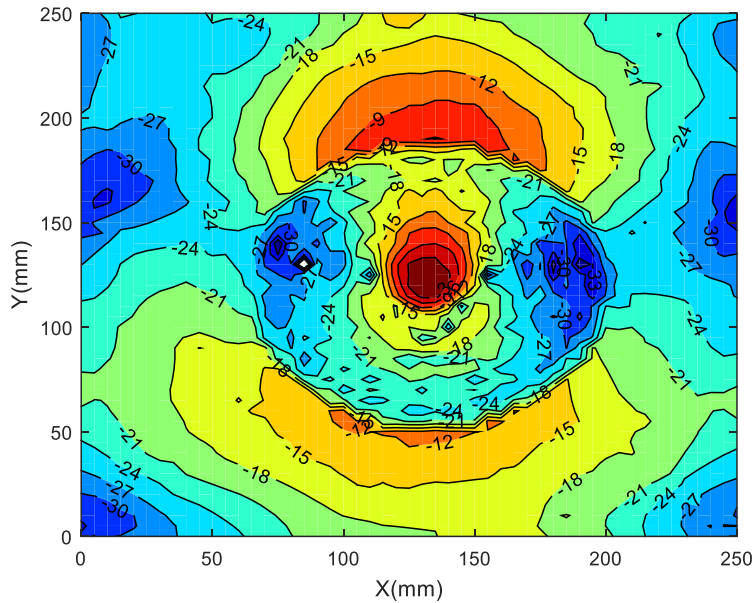
Figure 18: Contor plot of normalized power density at the middle of the breast

From Figure 18 it can be seen that electromagnetic field is highly concentrated in the middle of the plane and the width of the focused spot is very small. The width of the –3 dB spot at the center plane was found to be 15 mm x 20 mm.

For the use of this array for hyperthermia, a spherical tumor of 10 mm diameter was considered. The assumed contrast between malignant and normal breast tissue was 5:1 for the relative permittivity and 10:1 for the conductivity [60]. For our study, we assumed a dielectric permittivity of 59 and conductivity of 1.35S/m for the tumor. Figure 19 shows the contour plot of normalized power density at the location of the tumor. It can be seen that the width of the -3 dB region decreases, and the electromagnetic energy is closely confined to the width of the tumor region. The width of -3 dB region was found to be 5 mm x 15 mm. Hence, we can see that the 4x4 array produces a small focused spot at the tumor location.
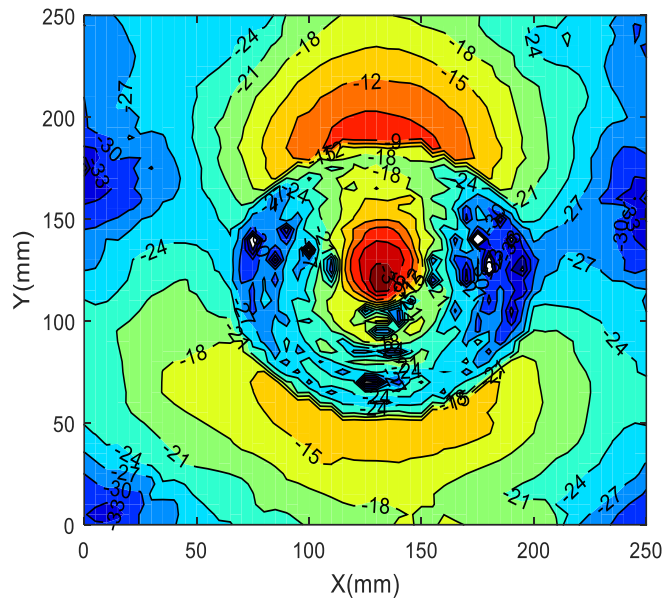
Figure 19: Contour plot of normalized power density at the center of the tumor

An off-center position of tumor was also considered, where the tumor was placed at a distance of 20 mm from the spherical breast surface in the positive Z direction. The location of the antenna array was adjusted or in other words the antenna array was moved backward along the Z direction such that the tumor is at the plane of maximum power density. Again, the power density was plotted at the center of the tumor tissue and it was seen that the power density was maximum at the center and is shown in Figure 20.
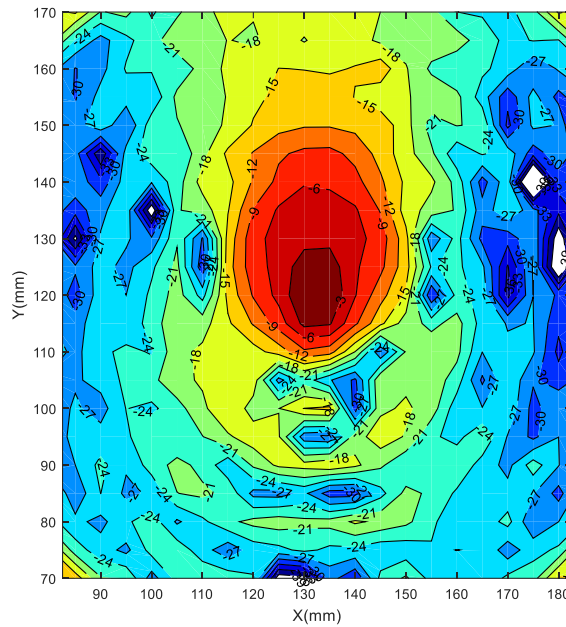
Figure 20: Contour plot of normalized power density at the center of the tumor for an off-center tumor position

Different placement locations of the antenna array were also studied. Rather than placing the antenna aperture facing the tip of the breast, the antenna was moved to the right side of the breast such that the aperture faces the spherical region of the breast. Power density plots were studied and regardless of the placement, the array was able to produce focused spot in the tumor region.

5.4.2. Hemispherical Breast model

With a spherical breast model, the antenna was able to produce a focused spot of the size of a typical Stage I breast tumor at the location of the tumor. In this section a hemispherical breast model was considered, and a similar analysis was done.

In [61] it is shown that, breast can be assumed to be hemispherical in shape, and can be modelled with four different layers closely simulating an actual breast [61]. The breast consists of a subcutaneous fat layer, followed by a gland layer and deep muscle layer. The sub cutaneous fat layer is covered by the outermost skin layer whose thickness is of the order of 3 mm. The muscle layer lies close to the thoracic wall. The thickness of the subcutaneous fat layer is 5 mm and thickness of the glandular layer and the muscle layer are 45 mm and 15 mm respectively. The thickness of the thoracic wall is 7 mm. A cross sectional model of a female breast is shown in Figure 21 below.
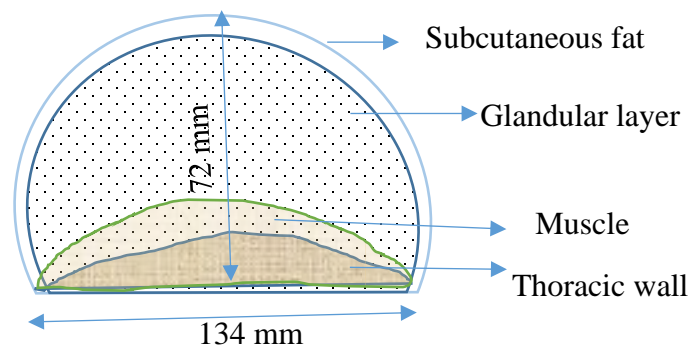
Figure 21: A two-dimensional cross-sectional model of female breast

Tumor cells are mostly located in the membranes of lobules and lactiferous ducts, and therefore for simulation purposes the tumor is typically placed in the glandular region of breast tissue [62]. The tumor can be modelled as a sphere of diameter 1 cm.

5.4.3. Results and discussion

The antenna array was first placed in front of the hemispherical breast and the distance between the array and the breast model is adjusted along the Z direction such that the position of maximum power density lies exactly on the center of the tumor. This is shown in Fig. 22 where

the antenna is at z=130 mm from the tumor center. Figure 23 shows the contour plot of normalized power density at the tumor location. As can be seen from the Figure, the power density is maximum at the center of the tumor and the width of the maximum power density region is very small, as desired.
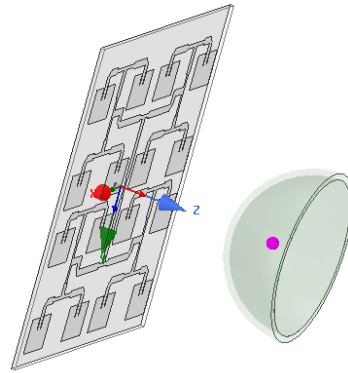
Figure 22:Antenna array placed in front of the breast tissue with tumor at the maximum power density position of the array
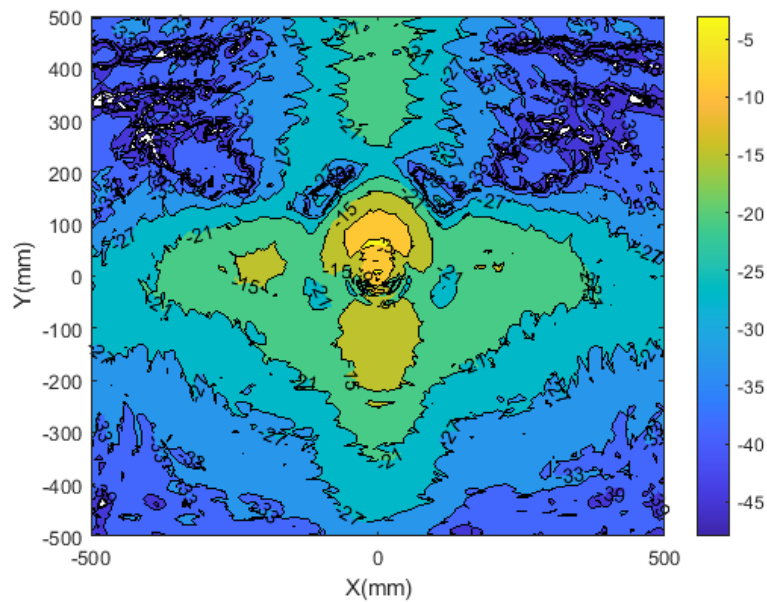
Figure 23: Normalized power density in the x-y plane at a distance of 130 mm with breast center and tumor center at z=130mm from the antenna aperture

In order to study the amount of energy absorbed in the tumor and the healthy breast tissue, the SAR values were studied. Fig.24 depicts the average SAR inside the breast tissue in the y-z plane with antenna facing the breast tissue. The maximum SAR value was found to be 3.66 W/Kg at the center of the tumor tissue and in the healthy tissue region surrounding the tumor tissue, the SAR value was less than the 2W/Kg limit set by FCC and ICNIRP guidelines [63]-[64]. The SAR value in the tumor indicates that the energy absorbed is high enough to destroy the cancer cells.
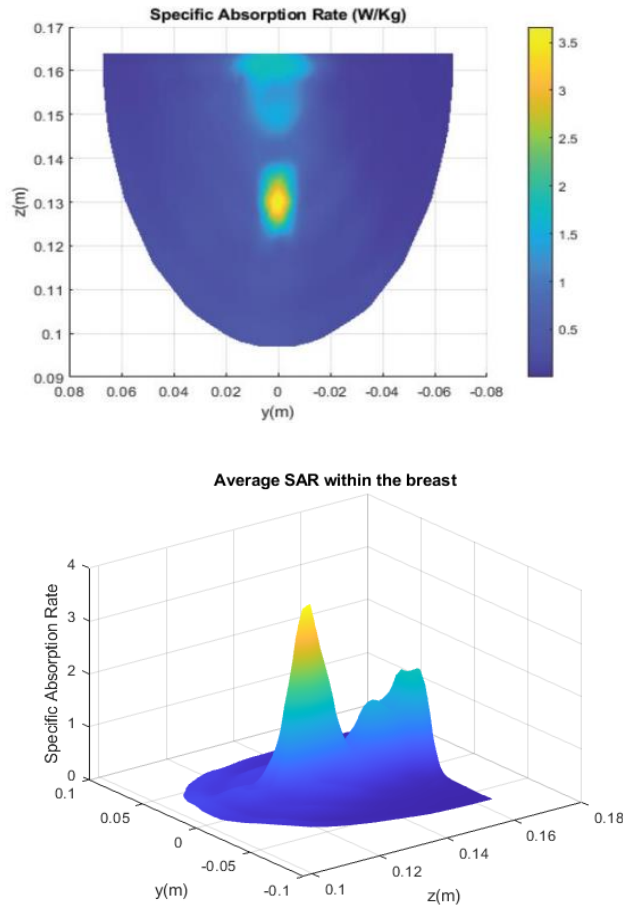
Figure 24: Average SAR within the breast tissue in the y-z plane with antenna array placed in front of the breast tissue

Next, with the tumor at the same location, the antenna array was moved to the left of the breast tissue at a distance z=130 mm from the tumor center as shown in Figure 25. The SAR results are shown in the y-z plane in Fig.26. Again, the maximum SAR was obtained at the center of the tumor tissue.

SAR Field
[W/kg]
1.5139E+000
1.0727E+000
7.6004E-001
5.3852E-001
3.8157E-001
2.7036E-001
1.9156E-001
1.3573E-001
9.6169E-002
6.8140E-002
4.8280E-002
3.4209E-002
2.4238E-002
1.7174E-002
1.2168E-002
8.6219E-003
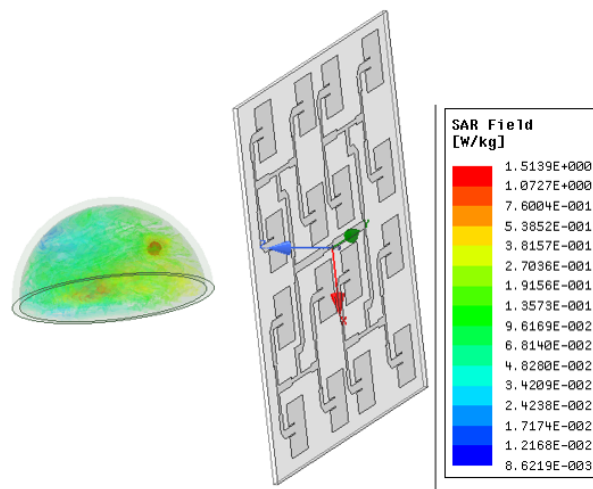
Figure 25: Placement of the antenna array on the left side of the breast tissue and the corresponding SAR field
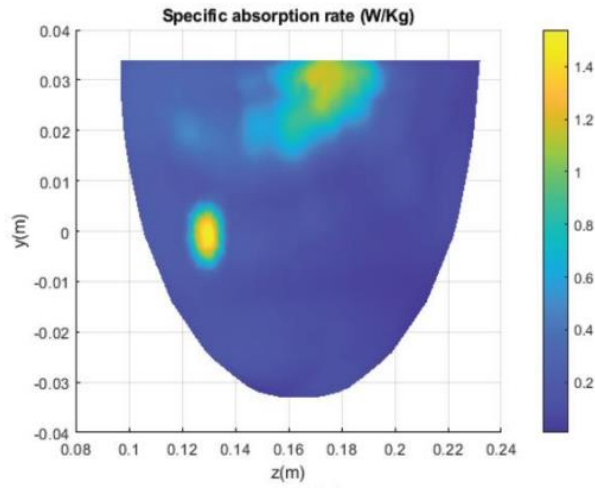
Figure 26: Average SAR within the breast tissue in the y -z plane with antenna array placed on the left of the breast tissue

To further study the suitability of this antenna array for hyperthermia treatment two different cases were investigated. Case I: changing the position of the antenna array in front of the breast with respect to the tumor location and Case II: changing the location of the tumor from the middle of the breast.

Case I: Changing the position of the antenna array in front of the breast with respect to the tumor location

The tumor was located at the center of the hemispherical breast and the antenna array was moved outward from z=130 mm, the position of maximum power density, in increments of 10 mm along the Z axis. The corresponding SAR value was noted at each position and is recorded in Table 7. This was done to see how crucial the location of the array and the corresponding maximum power density position is for the effective treatment of the tumor.

Table 7. Variation of SAR with movement of antenna array

Distance between antenna array and the center of the tumor	Maximum SAR and location of maximum SAR	SAR value at the chest wall
200 mm	3.18 W/Kg at tumor center	
190 mm	3.11 W/Kg at tumor center	
180 mm	3.01 W/Kg at tumor center	
170mm	2.76 W/Kg at tumor center	
160 mm	2.17 W/Kg at tumor center	
150 mm	3.54 W/Kg at tumor center	
140 mm	3.67 W/Kg at tumor center	
130 mm (location of maximum power density)	3.69 W/Kg at tumor center	
120 mm	3 W/Kg at tumor center	
110 mm	2.6 W/Kg at tumor center	
100 mm	2.2 W/Kg at tumor center	
90 mm	2.1 W/Kg at tumor center	82% of max. SAR close to chest wall
80 mm	1.94 W/Kg at tumor center	95 % of max. SAR close to chest wall
70 mm	1.95 W/Kg close to chest wall	1.8 W/Kg at tumor center
60 mm	1.99 W/Kg close to chest wall	1.52 W/Kg at tumor center

The SAR value at the tumor decreases as the antenna array is moved back and away from Z=130 mm, the maximum power density position, with the lowest value at a distance of 30 mm (z=160 mm). The value increases again for 40 mm, which corresponds to a distance of λg , which is the microstrip guided wavelength at 2.45 GHz. This value is, however, lower than that at z=130 mm. Hence it is seen that the SAR is the maximum, when the tumor lies at the maximum power density position. These results are shown in Fig. 27.

A similar trend was observed when the antenna array was moved more closer to the breast (moved forward along z axis) from the maximum power density position. The SAR decreases linearly as the antenna is moved forward closer to the breast and the value near the chest wall becomes greater than that in the tumor region. This can cause high temperatures near the chest wall and is not desired. Also, the width of the hot spot region in the tumor gets smaller than the diameter of the tumor, which implies that the energy absorbed in the tumor is not sufficient to completely heat the entire tumor.

Hence it is seen that as the antenna array is moved from the position of maximum power density (z=130 mm) in front of the breast, up to about +/- 20 %, the SAR is still high enough in the tumor for hyperthermia treatment while the SAR in the healthy tissue remains low.
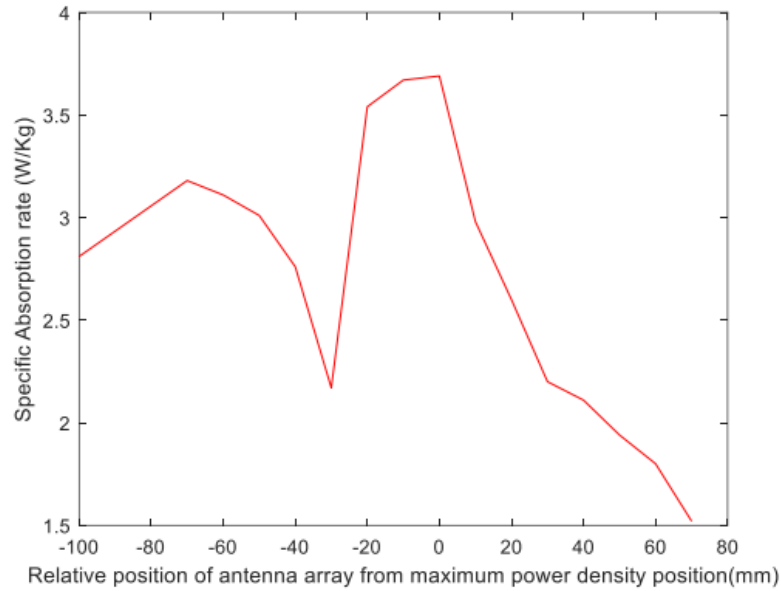
Figure 27: Variation of power density with movement of antenna array along the z axis

Case II: Changing tumor location within the breast

Three different locations for the tumor were considered for hyperthermia analysis: a) surface location b) deep location and c) off-center location. Surface position refers to positions 1-2 cm close to the surface of the breast and the deep tumor positions are farther from the center and closer to the chest wall at about $z = 150$ mm.

Surface tumor

For the case of surface tumor with the antenna at $z = 0$, the tumor was first placed at a distance of 1 cm from the breast tip at $z = 106$ mm. The SAR value was found to be the maximum of 2.02 W/Kg at the center of the tumor tissue. Near to the chest wall the SAR value was approximately 88 % of this maximum which is undesirable. In order to compensate for the change of the tumor location, to obtain the maximum power density at the tumor location, the antenna array was moved backwards. This caused an increase in the SAR value in the tumor tissue,

producing SAR of 2.23 W/Kg and the SAR near the chest wall was now 86 % of the maximum. Fig. 28 shows a contour plot of the SAR in the y-z plane for the surface tumor for this position of the antenna.
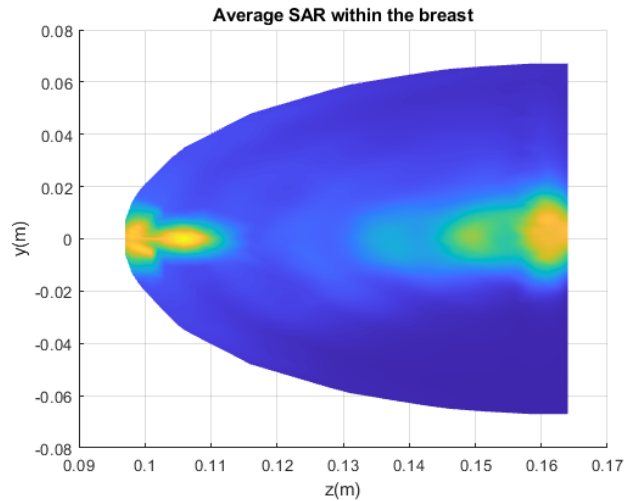
Figure 28: SAR plot in the y-z plane. (a). Tumor placed at a distance of 1 cm from breast tip and 106 mm from the center of the antenna array

Now we consider a surface tumor placed at a distance of 2 cm from the breast tip at z = 116 mm. The SAR value was found to be the maximum of 2.46 W/Kg at the center of the tumor tissue and near to the chest wall the SAR value was approximately 70 % of this maximum. Again, the antenna array was moved backwards to obtain the maximum power density at this tumor location. This caused an increase in the SAR value in the tumor tissue, producing SAR of 2.9W/Kg and the SAR near the chest wall was 67 % of the maximum. Fig. 29 shows a contour plot of the SAR in the y-z plane for this tumor location.
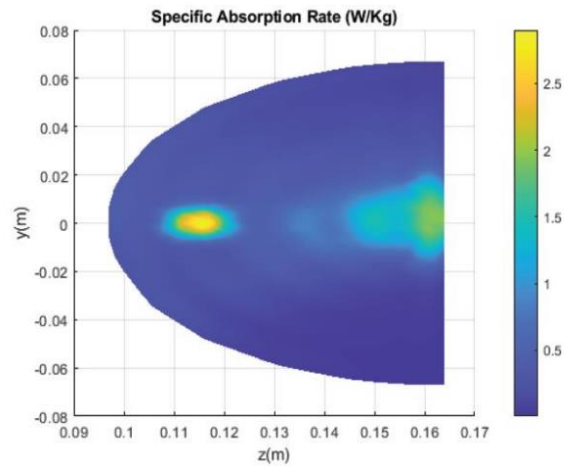
Figure 29: SAR plot in the y-z plane for surface tumor 2 cm from breast tip and 116 mm from the center of the array

Deep tumor

Here we consider the case of a tumor placed deep inside the breast at a distance of 5.4 cm away from the breast tip and 1.4 cm from the chest wall. The SAR value was found to be the highest at the center of the tumor, 7.64 W/Kg at z =151 mm. The diameter of the maximum SAR value region however was found to be 4-5 mm greater than the tumor diameter which indicates a heating up of the surrounding healthy tissue. Near to the chest wall SAR value was 52 % of the maximum. The antenna array was then moved forward, along the z direction, closer to the breast tissue so that the maximum power density position of the antenna array was at the center of the tumor. This caused the SAR value at the center of the tumor to be at 7.44 W/Kg and the SAR value at the chest wall was found to be 55 % of the maximum SAR value. Fig. 30 shows the contour plot of the SAR in the y-z plane for the deep tumor.
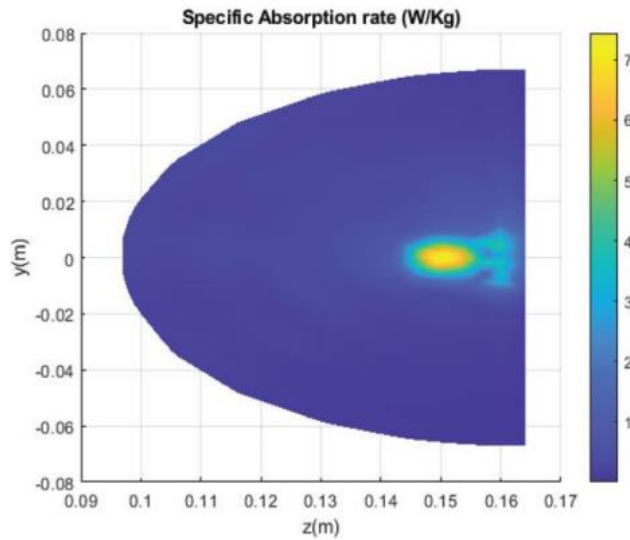
Figure 30: SAR plot in the y-z plane for deep tumor 1.4 cm from chest wall and 150 mm from the center of the array

It can be concluded that the array is capable of producing a high SAR region around a tumor irrespective of whether it's a surface tumor or deep tumor. This is achieved by properly moving the antenna array along the direction perpendicular to the antenna aperture to a location such that the maximum power density position of the antenna array coincides with the tumor location.

Tumor located at an off-center position

For surface tumor and deep tumor, the tumor was placed at the center (x=0, y=0) of the hemispherical breast. Here the tumor is moved to an off-center position. The antenna array was correspondingly moved such that the tumor is along the perpendicular (z direction) from the array and at the maximum power density plane. The tumor was located at (20 mm, 20 mm, 130 mm) and the center of the array was placed at (20 mm, 20 mm,0 mm). The corresponding SAR values obtained are shown in Fig. 31. The maximum SAR value of 1.67 W/Kg was found to be at the

60

center of the tumor and an additional hotspot that has a SAR value close to the maximum was found near the chest wall.
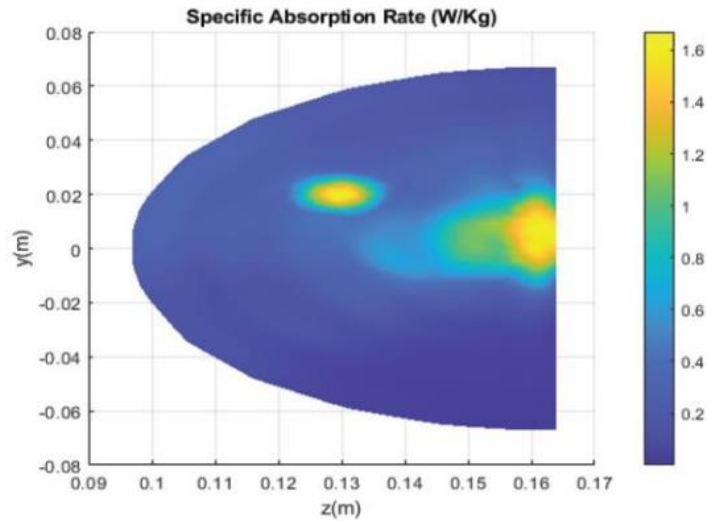
Figure 31: SAR plot in the y-z plane with tumor placed at an off-center location

5.5. Thermal simulations of the breast model with the tumor

From the electromagnetic analysis presented earlier, it was concluded that the antenna array was able to produce a focused spot with high SAR value at the location of the tumor. This high SAR value leads to an increased temperature in the tumor needed for hyperthermia treatment. To study the temperature elevation produced by the interaction of electromagnetic field with the breast tissue, thermal simulations were performed using SIM4LIFE software. SIM4LIFE uses finite difference time domain (FDTD) method to solve Pennes bioheat equation discussed in Chapter 3 Section 4. The equation considers metabolic body processes, blood circulation and the deposited energy from the externally applied electromagnetic field as heat sources. The generated heat spreads in the body by thermal diffusion.

61

The electromagnetic field generated from the EM analysis acts as the input source for the thermal simulations. The thermal properties of breast fat, breast gland and tumor tissues are listed in Table 8 [65].

Table 8. Thermal properties of breast tissue and tumor tissue at 2.45 GHz

Tissue	Density (kg/m^3)	Heat capacity (J/Kg/˚C)	Thermal conductivity (W/m.K)	Metabolic heat generation rate (W/Kg)	Heat transfer rate (W/m^3/K)
Breast fat	911	2770	0.21	0.73	2892.22
Breast gland	1041	3770	0.33	2.32	10542.6
Tumor	1050	3621	0.48	500	51000

Thermal analysis was done on the model with antenna array placed in front of the breast with tumor at the maximum power density position of z = 130mm from the array. The tumor was at the center of the breast. A target input power of 30 W was applied for a period of 60 minutes. The temperature profile inside the breast tissue at the center of the tumor in the x-y plane is shown in Figure 32. The temperature inside the green highlighted area represents, where the temperature is greater than 42 ˚C, needed for hyperthermia treatment and is over the entire tumor region. The healthy tissue remains at safer temperatures. Figure 33 shows the transient temperature at the location of maximum temperature inside the tumor. The temperature inside the tumor tissue

increases steadily and reaches a maximum of 44.7 ˚C inside the tumor in about 30 minutes and

thereafter remains at that steady state temperature.

(a)

(b)
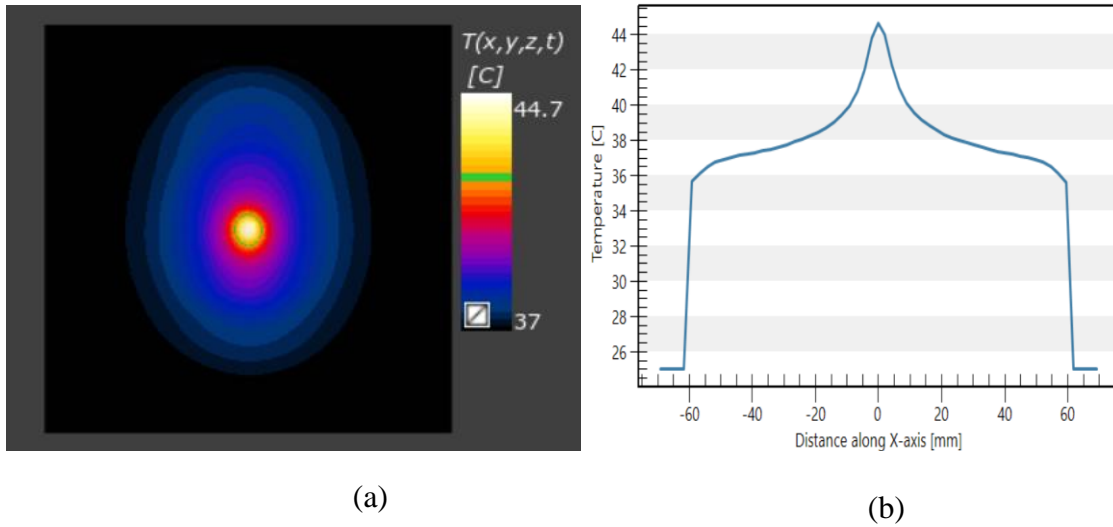
Figure 32: (a) Temperature profile in the x-y plane at the center of the tumor at z=130mm (b) Temperature plot inside the breast along x axis
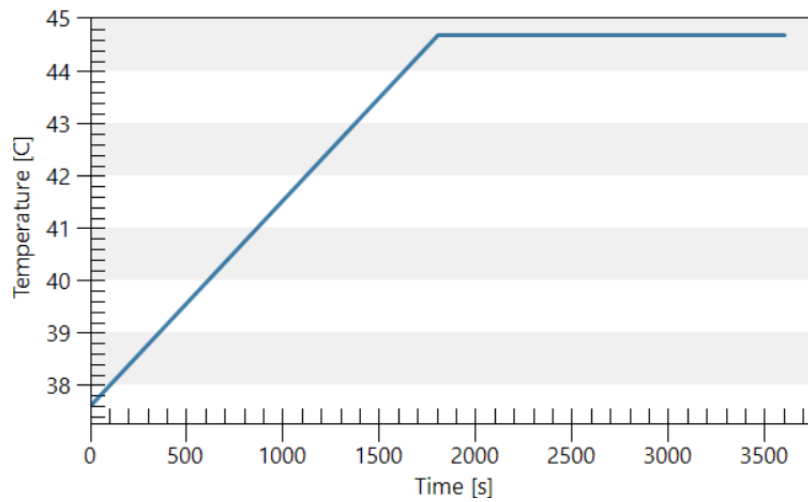
Figure 33: Transient temperature at the location of the maximum temperature inside the center of the tumor

The same analysis was done for a deep tumor location and a surface tumor location. For

the deep tumor, we consider the tumor to be located at z =150 mm, 14 mm close to the chest wall.

The antenna array was moved closer to the breast tissue along positive z direction so that the maximum power density position was at the center of the tumor. In order to produce temperatures greater than 42 ˚C, the target power was increased to 40 W for a duration of 60 minutes. The temperature inside the tumor reaches a maximum of 43.1 ˚C covering the entire tumor volume as can be seen in Figure 34. Figure 35 shows the variation of temperature with time at the location of maximum temperature.
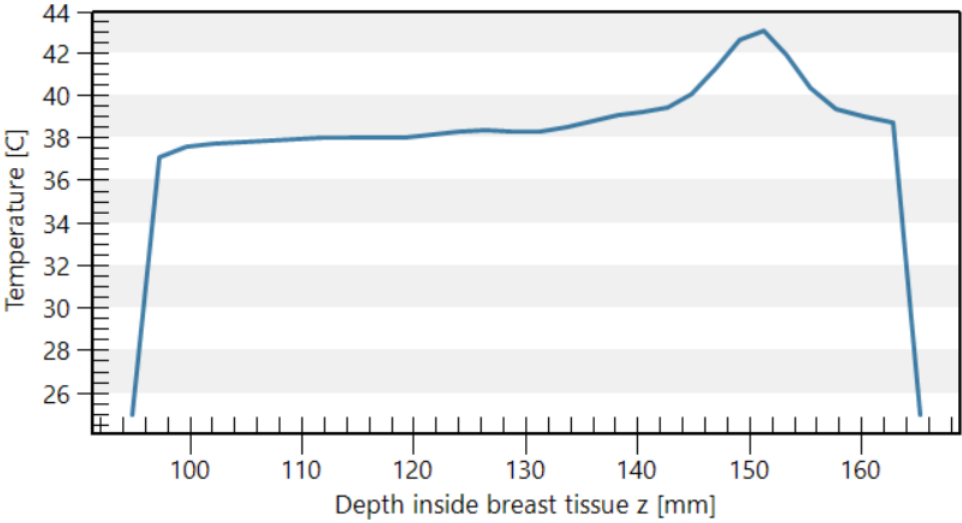
Figure 34: Temperature along z direction at x = y = 0 at the end of simulation period
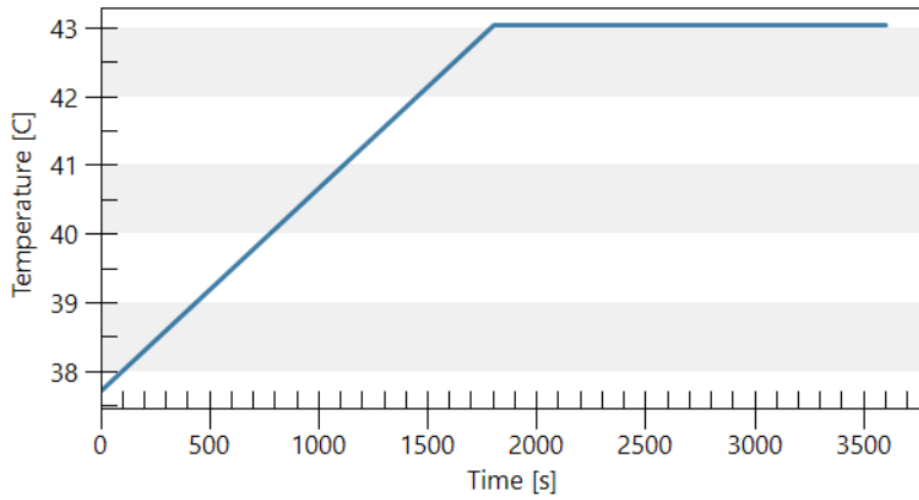
Figure 35: Transient temperature at the location of the maximum temperature inside the center of the tumor

For a surface tumor located at z = 116 mm, 20 mm away from the tip of the breast, the antenna array was moved farther along negative z direction such that the maximum power density position is at the center of the tumor. Figure 36 shows the temperature plot along the x direction at y = 0 and at the center of the tumor (z=116 mm) where maximum temperature was obtained. The temperature increases steadily and reaches a maximum value of 43.1 ˚C in about 30 minutes.
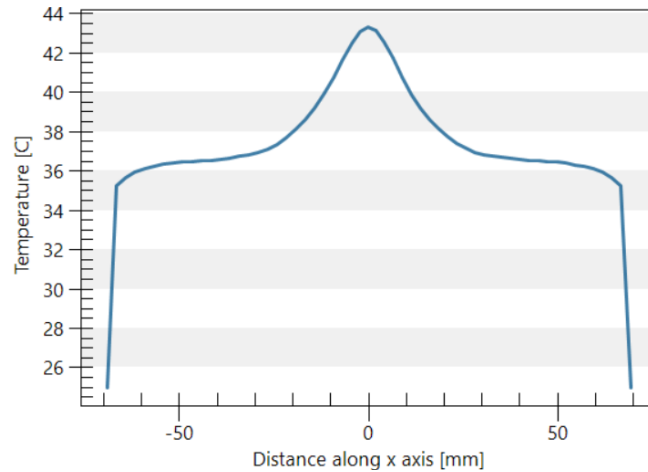
Figure 36: Temperature along x direction at y = 0 and z=116 mm at the end of simulation period

5.6. Conclusion

In this Chapter a near field focused planar microstrip antenna array was proposed for hyperthermia treatment of breast cancer. Near field focusing increases the electromagnetic power density in the near field region of the antenna array in a small region close to the antenna aperture. This focusing helps to improve temperature in a limited spot region around a diseased tissue, without causing any damage to the surrounding healthy tissue. Near field focusing was achieved using quadratic phase tapering along the antenna aperture. This is done by controlling the phases of the radiation source on the antenna aperture to compensate for the phase delay introduced by the path between each source and the corresponding focal point.

A two-layer heterogeneous hemispherical breast model consisting of low water content fat tissue and high-water content glandular tissue layer was used for the study. A spherical tumor of the size of a typical Stage I breast cancer was used for simulation studies. With the location of the tumor kept unchanged at the center of the breast, different location of the antenna array was

66

studied, and the SAR results confirm that the array can produce a focused spot at the location of the tumor. Different positions of the tumor were considered for both surface tumors and deep tumors. With proper positioning of the array, regardless of the position of the tumor, it was seen that the array could produce a focused spot at the location of the tumor. The antenna array can be placed on a rotating arm allowing it to be moved as needed.

Thermal simulations were done to study the increase in temperature inside the breast tissue due to the applied electromagnetic energy. The results of the simulations suggest that the antenna array can produce temperatures greater than 42 ˚C, needed for hyperthermia, inside the entire tumor volume, while keeping the healthy tissue at safer temperature.

CHAPTER 6: CONCLUSIONS

An important aspect of hyperthermia treatment is to raise the temperature of a tumor to a higher value while maintaining the temperature of the surrounding body tissue. The treatment method used must be capable of heating the entire tumor volume. These two challenges are addressed by using a near field focused antenna array for the treatment of breast tumor. Here a planar microstrip antenna array was used to raise the temperature of a spherical tumor located inside the breast tissue.

This dissertation explores two different antenna arrays for hyperthermia treatment. A grid antenna array and a near field focused antenna array were designed to operate at 2.45 GHz, for hyperthermia application. The limitation of grid antenna array to control the depth of focus was eliminated by using a near field focused antenna array. In near field focused array, the location of maximum power can be controlled by adjusting the phase of excitation of each individual antenna array element. Near field focused antenna can increase power density in a region close to the antenna aperture. The power absorbed by the tissue from the applied electromagnetic energy raises the temperature inside the tissue. Since tumors have reduced blood flow, the heat dissipation will be poor in the tumor. This makes the tumor more sensitive to the increased temperature and thereby destroying it.

A three dimensional, two-layer hemi-spherical breast model which closely resembles a normal adult female breast was considered for this study. The breast model considered for the study consists of low-water content fat layer and high-water content glandular tissue layer. A spherical tumor of the size of a typical Stage I breast cancer was studied.

68

With the near field antenna array placed in front of the breast tissue, the power density results were studied. Based on the location of maximum power density in free space, the antenna array is repositioned such that maximum power density plane lies at the center of the tumor. Studies were done to analyze, how crucial is the distance from the maximum power density position to the center of the tumor. With the distance between the antenna array and tumor kept the same, the array was moved to the left side of the breast tissue and the power density was still the maximum at the tumor. Different tumor positions were also studied to validate the results. This treatment method can be used when the position of the tumor is known in advance. Different placement location of the array was also studied and in each case the power density and specific absorption rate results were plotted. Thermal simulations were done to study the temperature increase inside the breast model due to the applied electromagnetic energy. The results of the simulation indicate the suitability of the antenna array for hyperthermia treatment

The method proposed here presented a noninvasive method of cancer treatment using hyperthermia. The designed antenna array can be attached to a rotating arm and can be positioned according to the location of the tumor to focus the energy onto the tumor. Simulation results suggests that the array was able to produce a focused spot at the location of the tumor without causing any damage to the surrounding healthy breast tissue.

REFERENCES

[1]   R. Chandra, H. Zhou, I. Balasingham and R. M. Narayanan, "On the Opportunities and Challenges in Microwave Medical Sensing and Imaging," in IEEE Transactions on Biomedical Engineering, vol. 62, no. 7, pp. 1667-1682, July 2015, doi: 10.1109/TBME.2015.2432137.

[2]   C. Johnson A. Guy, "Nonionizing Electromagnetic Wave Effects in Biological Materials and systems," IEEE Biolog. Effe. of Electrom. Radiation, pp. 47-73, 1983.

[3]   Lin, J.C. Microwave sensing of physiological movement and volume change: A review.Bioelectromagnetics 1992, 13, 557–565.

[4]   S. Y. Semenov and D. R. Corfield, "Microwave tomography for brain imaging: Feasibility assessment for stroke detection," Int. J. Antennas Propag., vol. 2008, pp. 254830-1–254830-8, 2008.

[5]   P. M. Meaney, K. D. Paulsen, A. Hartov and R. K. Crane, "Microwave imaging for tissue assessment: initial evaluation in multitarget tissue-equivalent phantoms," in *IEEE Transactions on Biomedical Engineering*, vol. 43, no. 9, pp. 878-890, Sept. 1996.

[6]   S. Curto, P. McEvoy, X. Bao and M. J. Ammann, "Compact Patch Antenna for Electromagnetic Interaction With Human Tissue at 434 MHz," in IEEE Transactions on Antennas and Propagation, vol. 57, no. 9, pp. 2564-2571, Sept. 2009.

[7]   H. P. Kok et al., "A 70 MHz double waveguide set-up for hyperthermia of deep superficial tumors," 2016 46th European Microwave Conference (EuMC), London, 2016, pp. 1219-1222.

[8]   M. Popovic and L. Duong, "Phased array for microwave hyperthermia: a preliminary study in a computational muscle phantom," *2005 IEEE Antennas and Propagation Society International Symposium*, Washington, DC, 2005, pp. 788-791 vol. 2B.

[9]   A. J. Greenspon, "Advances in catheter ablation for the treatment of cardiac arrhythmias," 2000 IEEE MTT-S International Microwave Symposium Digest (Cat. No.00CH37017), Boston, MA, USA, 2000, pp. 927-928 vol.2.

[10]   Siegel, R.L., Miller, K.D., Jemal, A.: Cancer statistics, 2018. CA Cancer J. Clin. 68(1), 7–30 (2018)

[11]   M.R. Horsman, J. Overgaard Hyperthermia: a potent enhancer of radiotherapy Clinical Oncology, 19 (6) (2007), pp. 418-426, 10.1016/j.clon.2007.03.015

[12]   Chang D, Lim M, Goos JA, Qiao R, Ng YY, Mansfeld FM, et al. Biologically Targeted Magnetic Hyperthermia: potential and Limitations. Front Pharmacol. 2018; 9:831.

[13]   Vorst André Vander, Arye Rosen, and Youji Kotsuka. RF/Microwave Interaction with Biological Tissues. Hoboken, NJ: John Wiley & Sons, 2006.

[14]   Gabriel S, Lau R W and Gabriel C 1996 The dielectric properties of biological tissues: III. Parametric models for the dielectric spectrum of tissues Phys. Med. Biol. 41 2271–93

[15]   Christ A, Samaras T, Klingenböck A and Kuster N 2006b Characterization of the electromagnetic near-field absorption in layered biological tissue in the frequency range from 30 MHz to 6000 MHz Phys. Med. Biol. 51 4951-66

[16]   A. Christ, A. Klingenbock, T. Samaras, C. Goiceanu and N. Kuster, "The dependence of electromagnetic far-field absorption on body tissue composition in the frequency range

from 300 MHz to 6 GHz," in IEEE Transactions on Microwave Theory and Techniques, vol. 54, no. 5, pp. 2188-2195, May 2006, doi: 10.1109/TMTT.2006.872789.

[17]   Gabriel C. (2000) The Dielectric Properties of Tissues. In: Klauenberg B.J., Miklavčič D. (eds) Radio Frequency Radiation Dosimetry and Its Relationship to the Biological Effects of Electromagnetic Fields. NATO Science Series (Series 3: High Technology), vol 82. Springer, Dordrecht. https://doi.org/10.1007/978-94-011-4191-8_10

[18]   M. A. Stuchly, S. S. Stuchly, "Experimental radio and microwave dosimetry," in *C. Polk and E. Postow (Eds.), Handbook of Biological Effects of Electromagnetic Fields, Bocaraton, FL:CRC Press,1996*

[19]   Zagar, Timothy M. et al. "Hyperthermia for Locally Advanced Breast Cancer." International journal of hyperthermia: the official journal of European Society for Hyperthermic Oncology, North American Hyperthermia Group 26.7 (2010): 618–624.

[20]   H. P. Kok and J. Crezee, "Hyperthermia Treatment Planning: Clinical Application and Ongoing Developments," in IEEE Journal of Electromagnetics, RF and Microwaves in Medicine and Biology, doi: 10.1109/JERM.2020.3032838.

[21]   H. Kato, J. W. Hand, M. V. Prior, M. Furukawa, O. Yamamoto and T. Ishida, "Control of specific absorption rate distribution using capacitive electrodes and inductive aperture-type applicators: implications for radiofrequency hyperthermia," in IEEE Transactions on Biomedical Engineering, vol. 38, no. 7, pp. 644-647, July 1991.

[22]   Y. Fujita, H. Kato and T. Ishida, "An RF concentrating method using inductive aperture-type applicators," in IEEE Transactions on Biomedical Engineering, vol. 40, no. 1, pp. 110-113, Jan. 1993.

[23] Deshan Yang et al., "A floating sleeve antenna yields localized hepatic microwave ablation," in IEEE Transactions on Biomedical Engineering, vol. 53, no. 3, pp. 533-537, March 2006.

[24] J. Stang, M. Haynes, P. Carson, M. Moghaddam, "A preclinical system prototype for focused microwave thermal therapy of the breast", IEEE Trans. Biomed. Eng., vol. 59, pp. 2431-2438, Sep. 2012.

[25] E. A. Lekka, K. D. Paschaloudis and G. A. Kyriacou, "Phased array design for near field focused hyperthermia based on reciprocity theorem," 2017 International Workshop on Antenna Technology: Small Antennas, Innovative Structures, and Applications (iWAT), Athens, 2017, pp. 277-280.

[26] X. He, W. Geyi, S. Wang, "Optimal design of focused arrays for microwave-induced hyperthermia", IET Microw. Antennas Propag., vol. 9, no. 14, pp. 1605-1611, 2015.

[27] R. A. Gardner, H. I. Vargas, J. B. Block, C. L. Vogel, A. J. Fenn, G. V. Kuehl, M. Doval, "Focused microwave phased array thermotherapy for primary breast cancer", *Ann. Surg. Oncol.*, vol. 9, pp. 326-332, 2002.

[28] S. Curto, P. McEvoy, X. Bao, M. J. Ammann, "Compact patch antenna for electromagnetic interaction with human tissue at 434 MHz", IEEE Trans. Antennas Propag., vol. 57, no. 9, pp. 2564-2571, Sep. 2009.

[29] W. Gee, S. Lee, N. K. Bong, C. Cain, R. Mittra, R. Magin, "Focused array hyperthermia applicator: Theory and experiment", IEEE Trans. Biomed. Eng., vol. BME-21, pp. 261-264, May 1983

[30] P. T. Nguyen, A. Abbosh, S. Crozier, "Microwave hyperthermia for breast cancer treatment using electromagnetic and thermal focusing tested on realistic breast models and antenna arrays", IEEE Trans. Antennas Propag., vol. 63, no. 10, pp. 4426-4434, Oct. 2015.

[31] M.M. Paulides, J.F. Bakker, N. Chavannes et al., "A patch antenna design for application in a phased-array head and neck hyperthermia application", IEEE Trans. Biomed. Eng., vol. 54, no. 11, pp. 2057-2063, 2007

[32] M. Tayel, T. Abouelnaga, A. Elnagar, "Pencil Beam Grid Antenna Array for Hyperthermia Breast Cancer Treatment System", *Circuits and Systems*, vol. 8, pp. 122-133, May 2017.

[33] Shih et al., C. Shih, P. Yuan, W.-L. Lin, H.-S. Kou, Analytical analysis of the Pennes bioheat transfer equation with sinusoidal heat flux condition on skin surface Med. Eng. Phys., 29 (2007), pp. 946-953

[34] P. Bernardi, M. Cavagnaro, S. Pisa and E. Piuzzi, "Specific absorption rate and temperature elevation in a subject exposed in the far-field of radio-frequency sources operating in the 10-900-MHz range," in IEEE Transactions on Biomedical Engineering, vol. 50, no. 3, pp. 295-304, March 2003.

[35] Furse, C., Christensen, D. A., & Durney, C. H. (2009). Basic introduction to bioelectromagnetics. Boca Raton, FL: CRC Press.

[36] Guidelines for limiting EMF exposure, International Commission on Non-Ionizing Radiation Protection, Health Phys., vol. 66, pp. 508-512, 1998.

[37] IEEE Standards for Safety Levels Respects to Human Exposure to Radio Frequency Electromagnetic Fields, 3 KHz to 300 GHz , IEEE C95.1-1991, 1992.

[38]   J. D. Kraus, "A backward angle-fire array antenna,"IEEE Transactions on Antennas and Propagation , AP-12,1,January 1964,pp.48-50

[39]   R. Conti, J. Toth, T. Dowling, and J. Weiss, "The wire grid microstrip antenna," IEEE Trans. Antennas Propag., vol. AP-29, pp. 157–166,1981.

[40]   Y. P. Zhang and M. Sun, "An Overview of Recent Antenna Array Designs for Highly-Integrated 60-GHz Radios," European Conference on Antennas and Propagation, March 23-27, 2009, pp. 3783-3786.

[41]   B. Zhang and Y. P. Zhang, "Analysis and synthesis of millimeter-wave microstrip grid array antennas," IEEE Antennas Propagat. Magn. vol.53, no. 6, pp 42-55, Dec. 2011.

[42]   Sun M., Zhang Y.P. (2016) Grid Antenna Arrays. In: Chen Z., Liu D., Nakano H., Qing X., Zwick T. (eds) Handbook of Antenna Technologies. Springer, Singapore

[43]   M. Tayel, T. Abouelnaga, A. Elnagar, "Pencil Beam Grid Antenna Array for Hyperthermia Breast Cancer Treatment System", *Circuits and Systems*, vol. 8, pp. 122-133, May 2017

[44]   X. Chen, G. S. Wang, K. Huang, "A Novel Wideband and Compact Microstrip Grid Array Antenna", IEEE Transactions on Antennas and Propagation, vol. AP-58, no. 2, pp. 596-599, February 2010.

[45]   M.Lazebnik, vD.Popovic, L.Mc Cartney, C. B.Watkins, M.J.Lindstrom,J.Harter,S.Sewall, T.Ogilvie,   A.Magliocco,   T.M.Breslin,   W.Temple,   D.Mew,   J.H.Booske, M.Okoniewski,and S.C.Hagness, "A large-scale study of the ultra wide band microwave dielectric properties of normal, benign and malignant breast tissues obtained from cancer surgeries," Physics in Medicine and Biology, vol. 52, pp. 6093-6115, 2007.

[46]   IEEE recommended practice for measurements and computations of radio frequency electromagnetic fields with respect to human exposure to such fields, 100 kHz–300 GHz, IEEE Standard C95.3-2002, (Revision of IEEE Standard C95.3-1991), 2002.

[47]   Semcad   X.,   SIM4LIFE,   SPEAG-Schmid   &   Partner   Engineering   AG, http://www.semcad.com.

[48]   Elkin EB, Hudis C, Begg CB, Schrag D. The effect of changes in tumor size on breast carcinoma survival in the U.S.: 1975-1999. Cancer. 104(6):1149-57, 2005

[49]   R. Hansen, "Focal region characteristics of focused array antennas," in IEEE Transactions on Antennas and Propagation, vol. 33, no. 12, pp. 1328-1337, December 1985, doi: 10.1109/TAP.1985.1143539.

[50]   A. Buffi, P. Nepa and G. Manara, "Design Criteria for Near-Field-Focused Planar Arrays," in IEEE Antennas and Propagation Magazine, vol. 54, no. 1, pp. 40-50, Feb. 2012, doi: 10.1109/MAP.2012.6202511.

[51]   P. Nepa and A.Buffi,"Near-field focused microwave antennas," IEEE Antennas and Propagation Magazine, vol.59, 2017

[52]   P. Nepa, A. Buffi, A. Michel, G. Manara, "Technologies for near-field focused microwave antennas," *Int. J. Antennas Propag.*, Mar. 2017.

[53]   J. T. Loane and S.-W. Lee, "Gain optimization of near field focusing array for hyperthermia applications," IEEE Transactions on microwave theory and techniques, vol. 37, no. 10, pp. 1629–1635, Oct. 1989.

[54]   L. Shan and W. Geyi, "Optimal Design of Focused Antenna Arrays," in *IEEE Transactions on Antennas and Propagation*, vol. 62, no. 11, pp. 5565-5571, Nov. 2014.

[55]   X. He, W. Geyi, and S. Wang, "Optimal design of focused arrays for microwave-induced hyperthermia," IET Microwaves, antennas and propagation, vol. 9, no. 14, pp.1605–1611, 2015.

[56]   F. Tofigh, J. Nourinia, M. Azarmanesh and K. M. Khazaei, "Near-Field Focused Array Microstrip Planar Antenna for Medical Applications," in IEEE Antennas and Wireless Propagation Letters, vol. 13, pp. 951-954, 2014.

[57]   C. A. Ballanis, Antenna Theory: Analysis and Design, 3rd ed. New York, NY, USA: Wiley, 2005, Ch. 14.

[58]   E. O. Hammerstad, "Equations for Microstrip Circuit Design," Proc. Fifth European Microwave Conf., pp. 268–272, September 1975.

[59]   J. Sherman, "Properties of focused apertures in the fresnel region," in *IRE Transactions on Antennas and Propagation*, vol. 10, no. 4, pp. 399-408, July 1962.

[60]   E. C. Fear, X. Li, S. C. Hagness and M. A. Stuchly, "Confocal microwave imaging for breast cancer detection: localization of tumors in three dimensions," in *IEEE Transactions on Biomedical Engineering*, vol. 49, no. 8, pp. 812-822, Aug. 2002.

[61]   Sudharsan, N. M., Ng, E. Y.-K, Teh, S. L. Surface temperature distribution of a breast with/without tumor Int. J. Computer Methods in Biomechanics and Biomedical Engineering, 1999, 2 (1), 187–199.

[62]   I. E. Khuda, "A Comprehensive Review on Design and Development of Human Breast Phantoms for Ultra-Wide Band Breast Cancer Imaging Systems", Eng. J., vol. 21, no. 3, pp. 183-206, Jun. 2017.

[63]   Federal Communications Committee, FCC, Office of Engineering and Technolog, OET, Evaluating Compliance, "FCC Guidelines for Human Exposure to Radiofrequency Electromagnetic Fields", Bulletin 65 (Edition 97-01), June 2001.

[64]   International Commission on Non-Ionizing Radiation Protection, ICNIRP, "ICNIRP Statement on the Guidelines for Limiting Exposure to Time-Varying Electric, Magnetic, And Electromagnetic Fields (Upto 300 GHz)", ed: Health Physics Society, 1998.

[65]   He Y, Shirazaki M, Liu H, Himeno R, Sun Z. A numerical coupling model to analyze the blood flow, temperature, and oxygen transport in human breast tumor under laser irradiation. Comput Biol Med. 2006 Dec;36(12):1336-50. doi: 10.1016/j.compbiomed.2005.08.004. Epub 2005 Nov 2. PMID: 16263105.